

Alma Mater Studiorum Università di Bologna  
Archivio istituzionale della ricerca

New insight into morphological and genetic diversity of *Phlyctema vagabunda* and *Neofabraea kienholzii* causing bull's eye rot on apple and pear

This is the final peer-reviewed author's accepted manuscript (postprint) of the following publication:

*Published Version:*

Neri F., Crucitti D., Negrini F., Pacifico D., Ceredi G., Carimi F., et al. (2023). New insight into morphological and genetic diversity of *Phlyctema vagabunda* and *Neofabraea kienholzii* causing bull's eye rot on apple and pear. *PLANT PATHOLOGY*, 72(2), 268-289 [10.1111/ppa.13662].

*Availability:*

This version is available at: <https://hdl.handle.net/11585/906629> since: 2022-11-23

*Published:*

DOI: <http://doi.org/10.1111/ppa.13662>

*Terms of use:*

Some rights reserved. The terms and conditions for the reuse of this version of the manuscript are specified in the publishing policy. For all terms of use and more information see the publisher's website.

This item was downloaded from IRIS Università di Bologna (<https://cris.unibo.it/>).  
When citing, please refer to the published version.

(Article begins on next page)

This is the final peer-reviewed accepted manuscript of:

Fiorella Neri, Dalila Crucitti, Francesca Negrini, Davide Pacifico, Gianni Ceredi, Francesco Carimi, Mauricio A. Lolas, Marina Collina, Elena Baraldi

*New insight into morphological and genetic diversity of Phlyctema vagabunda and Neofabraea kienholzii causing bull's eye rot on apple and pear*

*Plant pathology* Volume 72, Issue 2 February 2023 Pages 268-289

The final published version is available online at: <https://doi.org/10.1111/ppa.13662>

Terms of use:

This article may be used for non-commercial purposes in accordance with [Wiley Terms and Conditions for Use of Self-Archived Versions](#)

This item was downloaded from IRIS Università di Bologna (<https://cris.unibo.it/>)  
When citing, please refer to the published version.



**New insight into morphological and genetic diversity of  
Phlyctema vagabunda and Neofabraea kienholzii causing  
bull's eye rot on apple and pear**

Journal:	<i>Plant Pathology</i>
Manuscript ID	PP-22-147.R3
Manuscript Type:	Original Article
Date Submitted by the Author:	11-Oct-2022
Complete List of Authors:	<p>Neri, Fiorella; Alma Mater Studiorum University of Bologna, Department of Agricultural and Food Sciences (DISTAL)</p> <p>Crucitti, Dalila; Consiglio Nazionale delle Ricerche, Istituto di Bioscienze e BioRisorse (IBBR), Corso Calatafimi 414, 90129</p> <p>Negrini, Francesca; Alma Mater Studiorum University of Bologna, Department of Agricultural and Food Sciences (DISTAL)</p> <p>Pacifico, Davide; Consiglio Nazionale delle Ricerche, Istituto di Bioscienze e BioRisorse</p> <p>Ceredi, Gianni; Apofruit</p> <p>Carimi, Francesco; Consiglio Nazionale delle Ricerche, Istituto di Bioscienze e BioRisorse (IBBR), Corso Calatafimi 414, 90129</p> <p>Lolas, Mauricio; Universidad de Talca, Laboratorio de Fitopatología Frutal, Facultad de Ciencias Agrarias</p> <p>Collina, Marina; Alma Mater Studiorum University of Bologna, Department of Agricultural and Food Sciences (DISTAL)</p> <p>Baraldi, Elena; Alma Mater Studiorum University of Bologna, Department of Agricultural and Food Sciences (DISTAL)</p>
Topics:	epidemiology, taxonomy & phylogenetics
Organisms:	fungi
Other Keywords:	Fungal variability, mycelial cord, postharvest disease, $\beta$ -TUB2, ACT1, phylogeny

Running head: NERI et al.

**New insight into morphological and genetic diversity of *Phlyctema vagabunda* and *Neofabraea kienholzii* causing bull's eye rot on apple and pear**

Fiorella Neri<sup>1</sup>, Dalila Crucitti<sup>2,3</sup>, Francesca Negrini<sup>1</sup>, Davide Pacifico<sup>2</sup>, Gianni Ceredi<sup>4</sup>,  
Francesco Carimi<sup>2</sup>, Mauricio A. Lolas<sup>5</sup>, Marina Collina<sup>1</sup>, Elena Baraldi<sup>1</sup>

<sup>1</sup>*Department of Agricultural and Food Sciences, Alma Mater Studiorum - University of Bologna, Italy, via Gandolfi, 19, 40057 Cadriano Bologna, Italy*

<sup>2</sup>*Institute of Biosciences and Bioresources (IBBR), CNR, Corso Calatafimi 414, 90129 Palermo, Italy*

<sup>3</sup>*Department of Agricultural, Food and Forest Sciences (SAAF), University of Palermo, Viale delle Scienze, 90128 Palermo, Italy*

<sup>4</sup>*Apofruit, Viale della Cooperazione, 400, 47522 Cesena, Italy*

<sup>5</sup>*Laboratorio de Fitopatología Frutal, Facultad de Ciencias Agrarias, Universidad de Talca, Talca 3460000, Chile*

Fiorella Neri and Dalila Crucitti contributed equally to the paper.

Correspondence

Fiorella Neri; e-mail: [fiorella.neri@unibo.it](mailto:fiorella.neri@unibo.it)

## ORCID

Fiorella Neri 0000-0002-5144-9903

Dalila Crucitti 0000-0003-1860-5983

Francesca Negrini 0000-0003-1760-4778

Davide Pacifico 0000-0003-3620-9829

Francesco Carimi 0000-0002-7700-9527

Mauricio A. Lolas 0000-0002-5438-173X

Marina Collina 0000-0001-6980-7521

Elena Baraldi 0000-0001-9496-0093

## Keywords

$\beta$ -tubulin, *ACT1*, fungal variability, mycelial cord, phylogeny, postharvest disease

Fungi of genera *Phlyctema* and *Neofabraea* are the causal agents of bull's eye rot, a major postharvest disease of pome fruits. To investigate their morphological and genetic diversity, isolates obtained in Italy and Chile from decayed fruit and rainwater between 2014 and 2019 were grown on two agar media, inoculated onto four fruit cultivars and compared using four marker genes. Consistent intra- and interspecies phenotypic differences were recorded among isolates identified as *P. vagabunda* (two main morphotypes, PvM-I and PvM-II, were distinguished) and *N. kienholzii*. In particular, the Chilean isolates belonging to PvM-I showed low sporulation in vitro, while isolates belonging to PvM-II showed the most

abundant sporulation and also formed conidiomata deep within fruit tissue. Host cultivar influenced the disease incidence in unwounded, inoculated fruit. Cripps Pink and Golden Delicious apples favoured the formation of *P. vagabunda* conidiomata and macroconidia, while Granny Smith apples and/or Kaiser pears restricted sporulation of some isolates of PvM-I. Mycelial cords of *P. vagabunda* and *N. kienholzii* were consistently recorded in inoculated fruit, suggesting their possible involvement as a source of inoculum. Propagules of *P. vagabunda* were present in rainwater collected from apple plants from September to October in Italy. According to sequence analysis of ITS, *EF-1 $\alpha$* , *TUB2* and *ACT1* regions of the fungi, 12 distinct sequence types were identified, three of which were characteristic of isolates from the Southern hemisphere. The condensed maximum likelihood phylogenetic tree separated the 50 *P. vagabunda* isolates into six phylogroups, suggesting a correlation with their geographic distribution.

## 1 Introduction

Bull's eye rot, also known as lenticel rot, is one of the main postharvest diseases of pome fruits, producing notable economic losses during storage and shelf-life (Cameldi et al., 2017; Den Breeyen et al., 2020; Henriquez et al., 2004; Neri et al., 2009; Soto-Alvear et al., 2013; Spotts et al., 2009). Fruit infection initiates in the orchard, but the symptoms of disease appear after some months of cold storage, when the fruit have reached a certain stage of ripeness (Neri et al., 2019). The causal agents of bull's eye rot are fungal species belonging to the class of Leotiomycetes, which are currently assigned to the genera *Neofabraea* (*N. malicorticis*, *N. perennans* and *N. kienholzii*) and *Phlyctema* (Li et al., 2020). In many countries, the main causal agent of bull's eye rot is the species *Phlyctema vagabunda* (synonyms *Neofabraea vagabunda*, *N. alba*, *Pezicula alba* and *Gloeosporium album*)

reclassified and renamed several times in the past (Chen et al., 2016; Johnston et al., 2014; Verkley, 1999), while the species *N. kienholzii* has been recorded sporadically in recent years (Amaral Carneiro et al., 2022; Michalecka et al., 2016; Spotts et al., 2009). Due to the difficulty of inducing sporulation on common culture media, the morphological description of *P. vagabunda* in taxonomic studies has been based mainly on the in vivo growth, using few isolates for the in vitro description (Chen et al., 2016; Verkley, 1999). However, ambiguities or contrasting results have been reported in the literature regarding the diagnostic characters of *P. vagabunda*, in particular, the form of conidiomata, differently described as pycnidial (Bompeix, 1966; Li et al., 2020), sporodochial (Sutton, 1980), acervular (Gariépy et al., 2005; Soto-Alvear et al., 2013) or acervular to sporodochial (Chen et al., 2016), and the morphology of conidia (Cameldi et al., 2017; Chen et al., 2016; Li et al., 2020; Rooney-Latham et al., 2013; Soto-Alvear et al., 2013; Sutton, 1980; Verkley, 1999). Moreover, differences regarding the temperature requirement (Cameldi et al., 2017), the activity of degrading enzymes (Amaral Carneiro et al., 2022; Di Francesco et al., 2019) and symptoms induced in fruit, such as concentric zonation, the colour of lesions and the conidiomata size (Cameldi et al., 2017; Gariépy et al., 2005; Romero et al., 2018; Soto-Alvear et al., 2013) were recorded within *P. vagabunda*. Few illustrations of the macroscopic or microscopic characters of *P. vagabunda* are available to compare the results of the different studies (Amaral Carneiro et al., 2022; Cameldi et al., 2017; Chen et al., 2016; Gariépy et al., 2005; Sutton et al., 1980; Trouillas et al., 2019).

The high degree of phenotypic variability recorded in *Phlyctema* and *Neofabraea* spp. has not yet been thoroughly investigated at the genetic level. The limited sequence information available in the literature was mainly used to discriminate among the different species rather than within them (Cameldi et al., 2017; Chen et al., 2016; Den Breeyen et al., 2020; de Jong et al., 2001; Soto-Alvear et al., 2013). Previous attempts to define phylogenetic

relationships showed that  $\beta$ -tubulin provides the best separation among the *Neofabraea* species and also suggested its possible use to discriminate among *P. vagabunda* isolates (de Jong et al., 2001). A more recent study (Amaral Carneiro et al., 2022) confirmed the existence of intraspecies genetic variability among *Phlyctema* and *Neofabraea* isolates by means of multilocus sequence analysis of four genes (ITS, *EF-1 $\alpha$* , *TUB2* and mtSSU).

The present study aimed to (i) collect recent isolates of fungi causing bull's eye rot from decayed fruit and rainwater; (ii) describe the morphological features of the isolates on different culture media; (iii) characterize the morphological and pathological traits of representative isolates of the collection on hosts of different species (apple and pear) and susceptibility to bull's eye rot; and (iv) investigate the intraspecific variability within *Phlyctema* and *Neofabraea* spp. isolates using different genetic regions (ITS1, *EF-1 $\alpha$* , *TUB2* and *ACT1*).

## 2 Materials and methods

### 2.1 Collection of fungal isolates from fruit and rainwater

To establish a recent collection of isolates causing bull's eye rot, surveys were carried out on apple batches after some months of cold storage from 2014 to 2019 and rainwater was collected in the field in 2015 in Italy. The batches with decayed apples were inspected for the localization of symptoms of disease on fruit, the characteristics of lesions, and the appearance of conidiomata. To obtain a wide range of samples, fruit with typical symptoms of bull's eye rots (circular flat to sunken brown lesions with well-defined margin and wet conidiomata) and also fruit with atypical symptoms of the disease (i.e., atypical zonation, chlorotic halo surrounding lesion, occurrence of pigmented spots on lesions) were used to establish the

collection of fungi assayed in the present study (Figure S1). The main sources of collection were batches of Cripps Pink apple coming from commercial orchards in Italy (Apofruit, Emilia Romagna region), but also batches of other cultivars of apples (Fuji, Golden Delicious and Pinova) and of Cripps Pink apple coming from different growing areas of the other hemisphere (Chile) were included in the collection (Table 1).

To isolate the pathogen from fruit, small pieces ( $3 \times 3$  mm) of decayed tissue were taken from the margin of necrotic lesions, placed on tomato agar (TA: 500 g commercial Italian tomato puree, 15 g Oxoid agar technical and 500 ml distilled water) and maintained as monoconidial cultures on this medium at  $15^{\circ}\text{C}$  (Cameldi et al., 2017). To isolate fungi from rainwater, funnels were put at the base of five Cripps Pink apple plants of an experimental orchard of Bologna University (Cadriano, Italy) and bottles, fixed in the ground, collected water percolating from the plants. Water samples (40 ml each), collected after rainy days from May to November, were centrifuged in conic tubes at  $2800 \times g$  for 5 min to remove ground and other contaminants occurring in rainwater. The supernatant was diluted 1:1000 with distilled water containing 0.05% vol/vol Tween 80. Aliquots (100  $\mu\text{l}$ ) of diluted rainwater were distributed on the surface of potato dextrose agar (PDA) Petri dishes (90 mm diameter). The microbial colonies forming units were examined after 2, 3 and 5 days of incubation at  $20^{\circ}\text{C}$ , and those belonging to fungi were transferred onto TA Petri dishes and incubated in darkness at  $15^{\circ}\text{C}$ .

Mycelia of each isolate obtained from decayed fruit and rainwater were preserved on plugs of TA suspended in 15% glycerol solution and stored at  $-80^{\circ}\text{C}$ . The fungal isolates were revived on fresh agar media for in vitro and in vivo assays and molecular identification. A total of 51 fungal isolates were included in the study.

## 2.2 Molecular characterization

### 2.2.1 DNA extraction

For each isolate, approximately 100 mg of fungal mycelium were scraped from the surface of a TA dish using a sterilized scalpel and macerated by automatic high-speed stirring with 3 mm tungsten beads (TissueLyser II; Qiagen) for 2 min. The total DNA was purified following the CTAB method (Doyle & Doyle, 1987), eluted with 100 µl of nuclease-free water and stored at –20°C for further analyses. Concentration and purity of extracts were evaluated by spectrophotometric reading of absorbance at 260 and 280 nm (Synergy H4 microplate reader; BioTek).

### 2.2.2 Isolate identification and characterization

Isolates were identified by sequence analysis of partial ITS1, *EF-1α* and *TUB2* genetic regions. Specific PCR was carried out following amplification protocols reported in the literature using primer pairs from the original articles (Table 2). To investigate the intraspecific variability among *Phlyctema* and *Neofabraea* isolates further, sequence analyses were extended to other regions of *TUB2* and *ACT1* genes, using new primer sets designed in this study (Table 2). The new primers were selected following the alignment of genomic regions of other fungal species retrieved from GenBank (data not shown).

The PCR mixture (50 µl) contained 50–100 ng genomic DNA, 0.5 µl of each primer solution (10 µM), 5 µl dNTP Mix (2 mM), 5 µl DreamTaq Buffer 10×, 1.25 U DreamTaq DNA polymerase (Thermo Fisher Scientific Inc.), and nuclease-free water to final volume. PCR products were analysed by electrophoresis by 1% agarose gel electrophoresis in tris-borate-EDTA (TBE) buffer purchased as Bioline Crystal 10× TBE buffer (0.89 M Tris-Borate, 0.02 M EDTA, pH 8.3) along with a GeneRuler DNA ladder mix (Thermo Scientific) and visualized on a UV transilluminator after staining with GelRed nucleic acid gel stain (Biotium). PCR products were purified using the Thermo Scientific GeneJET Gel Extraction

and DNA Cleanup Micro Kit (Thermo Fisher Scientific Inc.) following the manufacturer's protocol. Raw sequence data were manually assembled and edited with MEGA X, with each base position sequenced at least twice. The BLAST function in the database of the National Centre for Biotechnology Information (NCBI) was used for sequence comparison and isolate identification. Sequences determined in this work were submitted to the NCBI, and accession numbers were assigned (Table 1).

The *ACT1*, *ITS1*, *EF-1 $\alpha$*  and *TUB2* sequences of each *P. vagabunda* isolate were trimmed to make the best fit, concatenated in single sequences and aligned with MUSCLE implemented in the software MEGA X (Kumar et al., 2018). The aligned sequences were then analysed via maximum-likelihood bootstrapping (ML-BS) using IQ-TREE v. 1.6.12 (Nguyen et al., 2015). The best-fit model of molecular evolution was determined for *ACT1* (TNe), *ITS1* (JC), *EF-1 $\alpha$*  (JC) and *TUB2* (TIM2+F), using ModelFinder (Kalyaanamoorthy et al., 2017) based on the Bayesian information criterion (BIC) scores (Chernomor et al., 2016). Then, a combined partition ML-BS analysis was conducted with IQ-TREE v. 1.6.12. Statistical support for the branches was evaluated by conducting a ML-BS bootstrap analysis of 5000 replicates. Sequences of *N. kienholzii* were chosen for rooting the tree.

### 2.3 Morphological characterization and growth rate assay

To describe the in vitro morphology of the pathogens, the isolates identified as *P. vagabunda* and *N. kienholzii* were incubated in darkness on TA at 15°C on 90 mm Petri dishes (Cameldi et al., 2017) for 90 days, and the main features of the aerial mycelium (texture, shape, colour, growth, exudates and hyphal branching), conidiomata (time of appearance, position in agar medium, colour and shape) and conidia (size, shape, site of formation and amount) were recorded. To observe the pattern of growth, the largest and smallest colony diameters were measured at regular intervals until full growth and the mean data were calculated. The colony

growth rate (mm/day) was calculated after 21 days of incubation, when most isolates showed the maximum daily growth. The colony morphology was observed under a stereomicroscope Nikon SMZ-10 after 14, 30, 60 and 90 days of incubation. The microscopic traits of cultures were observed under a light microscope Eclipse E600 (Nikon Instruments) equipped with 10×, 20× and 40× objectives. A DXM1200 digital camera (Nikon Instruments) was used to capture digital images of the cultures. Fungal specimens examined under the microscope were mounted in sterile water on a glass slide. Samples for microscopic observation were prepared after washing 30-day-old colonies (eight plugs, 6-mm in diameter, were agitated for 30 s by vortex in tubes with 5 ml distilled water and 0.05% vol/vol Tween 80) and also by the slide pressure technique (a microscope slide was pressed on the colony, turned over and covered with a cover slip) after 30, 60 and 90 days of incubation. Five replications of each isolate were evaluated and the experiment was repeated at least twice.

The macroscopic and microscopic characters of 44 isolates of *P. vagabunda*, which were not affected by storage at  $-80^{\circ}\text{C}$ , and of the isolate NK1 of *N. kienholzii* were also examined during culture on PDA, at the same conditions of light and temperature described above.

## **2.4 Pathogenicity tests**

### **2.4.1 Wounded fruit**

The pathogenicity of the isolates identified as *P. vagabunda* or *N. kienholzii* was verified in preliminary assays carried out on wound-inoculated Cripps Pink apples. To obtain a sufficient number of conidia suitable for fruit inoculation, each fungal isolate was cultured on three TA Petri dishes and incubated at  $15^{\circ}\text{C}$  in the dark for 30 days. Conidial suspensions were prepared by washing these cultures with sterile distilled water containing 0.05% vol/vol Tween 80. Conidial concentrations were determined with a haemocytometer and adjusted to

10<sup>4</sup> conidia/ml. Twenty microlitres of these suspensions were used to inoculate 20 fruit per isolate wounded (2 × 2 × 2 mm) in the equatorial zone, with a sterile needle (one wound per fruit). Inoculated fruit were left at room temperature to allow complete water evaporation, then stored at 0°C. Fruit inoculated with distilled water were used as a control.

Subsequent assays were carried out on three cultivars of apple (Golden Delicious, Granny Smith and Cripps Pink) and one cultivar of pear (Kaiser) to compare the pathogenicity and symptomatology of 14 isolates of *P. vagabunda* (F1, F4, F8, F13, F14A, F19, F60, ID02, PFUTalca27, PNV1, RS1, RS2, RS4 and ZOF3), representative of the collection, and the isolate NK1 of *N. kienholzii*.

Fruit lots of these cultivars were wound-inoculated with conidial suspensions of these isolates, using the methodology previously described, then stored at 0°C. The incidence of infected wounds and the diameter of lesions (mm) were recorded 40, 60, and 90 days postinoculation (dpi) in pears and 60, 90, and 120 dpi in apples, and the disease symptoms were observed until the formation of mummies. The sample unit was represented by three repetitions of 20 fruit each per cultivar and fungal isolate.

#### **2.4.2 Unwounded fruit**

To better simulate the natural conditions of infection, further assays of artificial inoculation were carried out on unwounded fruit of the same cultivars, using the isolates F1, F8 and ID02 of *P. vagabunda*, which had a high sporulation rate in vitro, and the isolate NK1 of *N. kienholzii*. Five Petri dishes of each isolate were washed with sterile distilled water containing 0.05% vol/vol Tween 80, and conidial suspensions with concentrations of 10<sup>5</sup> conidia/ml were prepared as previously described; this concentration had proved to be suitable for successful infection of intact fruit in previous trials. Fruit were uniformly sprayed with 8 ml per fruit of these conidial suspensions. The inoculated fruit were left at room

temperature to allow complete water evaporation, then stored at 0°C and examined for the progression of bull's eye rot symptoms until the formation of mummies (12–18 months depending on host and isolate).

## 2.5 Statistical analysis

The data of in vivo assays were subjected to one-way analysis of variance (ANOVA) using the statistical package STATISTICA FOR WINDOWS (Statsoft Inc.). Separation of means was performed using Tukey's test ( $p < 0.05$ ).

## 3 Results

### 3.1 Identification of fungal isolates from fruit and rainwater

All primer pairs retrieved from the literature amplified fragments of expected sizes. The new primer pairs designed from the alignment of *ACT1* and *TUB2* gene from fungal species other than *Neofabraea* produced fragments of about 1.1 kb (Table 2). Based on multilocus sequence data 47/48 fungal isolates obtained from tissue of decayed apple fruits were identified as *P. vagabunda*, one as *N. kienholzii* (Table 1).

Microscope observations of rainwater percolating from Cripps Pink apple plants from May to November recorded the presence of fungal spores in all samples examined and the occurrence of mycelial cords (about 400–700  $\mu\text{m} \times 11\text{--}28 \mu\text{m}$ ) in the samples of May, June, September, October and November. The distribution of diluted aliquots of rainwater on TA plates enabled the isolation of single fungal colonies, and the molecular analyses carried out on monoconidial cultures of the main fungal species recorded identified the presence of *P. vagabunda* in the samples of rainwater collected from September to November. Three isolates of *P. vagabunda* obtained from rainwater (FRNV1, FRNV2 and FRNV3) were

included in this study for subsequent morphological, pathological and molecular characterization (Table 1).

### 3.2 Morphological characterization in vitro

A great diversity in the morphological characters of colonies, conidiomata and conidia was recorded among the isolates of *P. vagabunda* tested in vitro. According to these characteristics, the isolates of this species were grouped into two main morphotypes (Cameldi et al., 2017) and the isolates of morphotype I of *P. vagabunda* (PvM-I) were further divided in four subclades (A–D) for growth on TA and PDA (Tables S1 and S2; Figure S2).

Consistent differences in morphology were recorded between the isolates of *P. vagabunda* and *N. kienholzii* in both agar media.

### 3.3 Description of *P. vagabunda* and *N. kienholzii*

#### 3.3.1 On TA

The colour of *P. vagabunda* colonies grown on TA ranged from pale cream to toasted almond-cinnamon with dark brown concentric rings, and sometimes differed among the replicates from the same inoculum or among the experiments. The maximum colony diameter varied from 50.3 to 73.7 mm, depending on isolate (66.3 mm on average) and was reached after about 5–7 weeks of incubation (Table S1; Figure S2). Out of 50 isolates examined in total on TA, 90% were similar to PvM-I. The isolates of this morphotype formed circular or oblong colonies, with more profuse development of aerial mycelium and more rapid growth rate (1.9 on average after 21 days of incubation) than the isolates of *P. vagabunda* morphotype II (PvM-II) on TA (1.6 mm/day).

Drops of hyaline and transparent exudates (water-like) adhering to the hyphal surface, initially recorded in young cultures of *P. vagabunda* and especially in isolates of PvM-I,

became denser with age (Figure 1a,b). Pigmented exudates (from amber to dark brown) were recorded on the top or around the aerial hyphae of mature colonies of some *P. vagabunda* isolates (Table S1; Figure 1c,d). The slide pressure technique, applied 30 days postincubation on TA, showed the formation of highly branched hyphae in the majority of isolates belonging to PvM-I. These specialized hyphae were mainly located in the outer part of the colony and formed the shape of a broken comb, a fern leaf surface, or coral (Figure 1e–h; Table S1). After 14–30 days' incubation on TA, most isolates of PvM-I (PvM-IA, IB and ID) formed only short (<15 µm long), straight, or weakly curved conidia, with rounded or slightly pointed apices (Figure 1i), arising from linear (Figure 1j) or branched hyphae (Figure 1 k–m) of the aerial mycelium. Black or pink mycelial cords, up to 15 mm long, formed by aggregation of linear or twisted hyphae, often reinforced by anastomoses or wrapped by peripheric hyphae growing around the main filament, were recorded on the surface of mature colonies (30–90 days old) of many isolates belonging to PvM-I, often located beside conidiomata (Figure 1n–t). Most isolates belonging to PvM-I formed only (PvM-IA, 38%) or mainly (PvM-IB and IC, 44%) superficial conidiomata (globose to subglobose, from 100 to 500 µm in diameter, initially closed), which were detachable when colonies were washed after 30 days' incubation (Table S1; Figure 1u). They were visible to the naked eye in aggregates (from 2 to 4.5 mm in diameter) or scattered, emerged on TA medium or semi-immersed after 35–60 days' incubation, depending on isolate (Table S1). These conidiomata were yellowish or yellowish and brown, more rarely only brown (PFUTalca27, F19, F61 and F68), covered with transparent to cream-amber exudates (less frequently dry), glabrous or covered by short hyphae (Figure 1v–y). The isolates grouped in PvM-ID (PFUTalca24, PFUTalca25, PFUTalca27 and PFUTalca37) also formed conidiomata immersed in agar medium in 60 day-old-colonies, which were visible after the removal of the aerial mycelium (Figure 1z). Conversely, the isolates belonging to PvM-II (F10, F13, F14A, ID02 and

FRNV1) formed oblong-piriform (from 50 to 400  $\mu\text{m}$  in diameter) conidiomata immersed in the agar medium (Figure 1 a1–a4), which were not detachable by washing of colonies after 30 days' incubation. They could be noticed early (after 14 days' incubation) by the release on colony surfaces of drops (initially small, then enlarging and merging in 60-day-old colonies) of sticky, waxy, cream-amber to dark brown mucilage containing masses of long, allantoid conidia ( $22\text{--}26 \times 3\text{--}4 \mu\text{m}$ ) liberated by the rupture of the conidiomata wall (Figure 1 a5,a6). In addition, some isolates grouped in PvM-IC formed both micro and macroconidia after 30 days' incubation. Guttules were often recorded in allantoid macroconidia, while only a sporadic occurrence of this feature was observed in microconidia of *P. vagabunda*. Late formation of conidia from open conidiomata was recorded in some isolates of PvMs-1A-C after 60–90 days' incubation on TA, detectable by the release of amber-dark gelatinous drops of mucilage by the conidiomata. After 30 days' incubation, all isolates of *P. vagabunda* were able to sporulate, allowing preparation of conidial suspensions with concentrations of  $3 \times 10^5$  conidia/ml on average by colony washing (Table S1). However, marked deviations from this rate of sporulation were recorded for the isolates PFUTalca24, PFUTalca25 and PFUTalca37, which showed about 100-fold lower sporulation, and for the isolates belonging to PvM-II (F10, F13, F14A, ID02 and FRNV1), which showed about 100-fold greater sporulation on this agar medium.

The growth rate on TA of the isolate NK1 of *N. kienholzii* (1.5 mm/day after 21 days' incubation on TA) was slower than all isolates of *P. vagabunda*, and the maximum radial growth of NK1 on TA (64 mm) was reached after 45 days of incubation on this medium (Table S1). This isolate was characterized by the formation of white, filamentous, radiating colonies on TA, markedly umbonate, with copious development of aerial mycelium, few radial grooves, and many feathery fascicles of aerial hyphae near the centre and extending towards the lid (Figure 2a,b). Drops of hyaline exudates adhering to hyphal surfaces, initially

transparent (water-like) and later becoming denser, were observed on the top of NK1 cultures (Figure 2c,d). Black (more rarely pink) mycelial cords were recorded early on the top of young colonies (14 days old) and also below the aerial hyphae of 60-day-old colonies of this *N. kienholzii* isolate (Figure 2e–k); in addition, tangles of mycelial cords were sometimes visible on the surface of mature colonies (Figure 2l). After 30 days' incubation, abundant formation of conidia by the aerial mycelium of *N. kienholzii* (Figure 2m) was recorded, both from linear (Figure 2n) and branched hyphae (Figure 2o,p). Brown conidiomata immersed in TA were visible in 40-day-old colonies after the removal of the aerial mycelium (Figure 2q,r), and yellow, sticky drops of slime conidia were observed on the colony surface of NK1 after 75 days' incubation (Figure 2s–u). Emerged and semi-immersed conidiomata, covered with exudates, generally appeared on the surface of colonies of *N. kienholzii* after 90 days' incubation (Figure 2v–x).

### 3.3.2 On PDA

The majority of the *P. vagabunda* isolates cultured on PDA formed colonies with irregular shape and margins (from undulating to dendritic). They also grew more slowly on PDA than on TA (mycelial growth rate of 1.2 mm/day after 21 days' incubation on average, Table S2 and Figure S2), and, in particular, the isolates of PvM-II (F10, F13, F14A, FRNV1 and ID02) showed the slowest growth on this medium (0.7 mm/day on average). Conversely, the isolate F19 formed circular colonies with even margins on PDA. Less aerial mycelium was formed by *P. vagabunda* on PDA than TA, and the isolates PNV1 and RS1, belonging to PvM-IC, also showed a profuse inner growth of the mycelium on PDA. The formation of tubular fascicles of aerial hyphae (1–2.5 mm long) displayed in circular rings characterized some isolates of *P. vagabunda* grouped in subclade IB and IC (Table S2). The colour of colonies on PDA varied greatly among the isolates of PvM-I, from white-pale pink in the isolates grouped in the subclade IA to brown in the centre with a cream margin in the isolates

grouped in the subclade IB, while the isolates of PvM-II (F10, F13, F14A, ID02 and FRNV1) formed pale cream colonies that were brown-salmon in the centre. Many isolates of *P. vagabunda* grown on PDA formed pigmented exudates on hyphae (from amber to dark brown) and released a diffusible dark pigment which stained the agar medium (Table S2 and Figure S2).

Most isolates of *P. vagabunda* grown on PDA only or mainly formed emerged conidiomata, visible on colony surfaces after 40 or 60 days' incubation (Table S2 and Figure S2). Conversely, the isolates of PvM-ID (PFUTalca24, PFUTalca25, PFUTalca27 and PFUTalca37) mainly formed conidiomata immersed in the medium in 60-day-old colonies (visible by the removal of mycelium) and few conidiomata on colony surfaces; in addition, the isolates belonging to the PvM-II (F10, F13, F14A, FRNV1 and ID02) only formed conidiomata immersed in the medium. In general, less abundant sporulation was recorded from *P. vagabunda* isolates cultured on PDA than on TA (−64.4% on average), and about 20% of isolates of PvM-I (PFUTalca27, PFUTalca32, F3, F8, F17, F27, GRG3, PNV1 and RS2) were unable to form conidia after 30 days' incubation on PDA. Only the isolates belonging to PvM-II (F10, F13, F14A, FRNV1 and ID02) and the isolate RS1 belonging to PvM-IC showed waxy drops of slimy conidia (salmon-coral to brown) on the surface of PDA colonies after 30 days' incubation. The conidia formed by the PvM-I of *P. vagabunda* on were short and straight, while those formed by the PvM-II (ID02, F10, F13, F14A, FRNV1) were long and allantoid. Only the isolate RS1 of PvM-IC formed macroconidia on PDA; however, the conidia formed by this isolate on PDA were thinner than those formed on TA. No specialized branched hyphae were recorded during growth of *P. vagabunda* on PDA, and only few mycelial cords were formed by some isolates of the PvM- I on this substrate.

The isolate NK1 of *N. kienholzii* incubated on PDA formed circular, white-pale pink colonies, having less abundant development of aerial mycelium than on TA (Table S2 and

Figure S2). However, NK1 had more rapid radial growth on PDA than on TA, reaching a growth rate of 1.8 mm/day after 21 days' incubation, and formed colonies with a maximum diameter of 70.3 mm after 6–7 weeks' incubation on PDA. No mycelial cords or specialized branched hyphae were recorded during growth of NK1 and significant reduction of sporulation was also observed for this isolate on PDA in comparison to TA (about 100-fold less); however, no differences in shape and size were observed between NK1 conidia formed on PDA or TA. NK1 formed immersed conidiomata earlier (after 40 days of incubation), while emerged and semi-immersed conidiomata appeared on colony surfaces after 90 days' incubation on PDA.

### 3.4 Phylogenetic analysis

Concatenated DNA sequences of 3065 bp from 50 *P. vagabunda* isolates, composed of ITS1, *EF-1 $\alpha$* , *TUB2*, and *ACT1* fragments of 516, 409, 1022 and 1118 bp, respectively, were aligned to generate a condensed ML phylogenetic tree with *N. kienholzii* isolate NK1 as outgroup (Figure 3). Sequence alignment revealed a single nucleotide (T) repeat (of six, five or four Ts) in the ITS1 region, 17 and two single nucleotide polymorphisms (SNPs) in the *TUB2* and *ACT1* regions, respectively, and no sequence variants in the *EF-1 $\alpha$*  region. Overall, these mutations distinguished 12 sequence types (1–12) (Figure 4 and Table 1) distributed in six phylogroups (I–VI) supported by bootstrap values higher than 70% (Figure 3). The Italian isolates of *P. vagabunda* clustered in four phylogroups (I, II, V and VI), containing nine sequence types, while the Chilean isolates clustered in two phylogroups (III and IV) containing three specific sequence types.

Four out of six phylogroups (I, II, III and VI) included *P. vagabunda* isolates characterized by different phenotypic traits in vitro, while only two phylogroups (IV and V) included isolates characterized by the same morphotype (ID and IC, respectively; Table S3).

PvM-IA was prevalent in phylogroups II and VI but absent in phylogroup I, PvM-ID was prevalent in phylogroup III, and PvM-II was recorded only in phylogroup I.

### 3.5 In vivo assays

#### 3.5.1 Wounded apples and pears

Assays carried out in different years of experimentation on wound-inoculated Cripps Pink apples proved all isolates of *P. vagabunda* and *N. kienholzii* included in this study could cause disease symptoms 60 dpi; however, some differences, regarding the type of conidiomata formed by the isolates, were recorded 180 dpi (data not reported). To examine the in vivo characteristics of the isolates in more depth, comparative assays were carried out on different cultivars of pome fruits (Cripps Pink, Golden Delicious apples and Kaiser pears, highly susceptible to bull's eye rot, and Granny Smith apples moderately resistant to this disease), using 14 isolates representative of the *P. vagabunda* collection and the isolate NK1 of *N. kienholzii*. For both pathogens, the first symptoms of disease in wound-inoculated fruit manifested at 40 dpi in pears and 60 dpi in apples, and consisted of a firm, darkened area around the site of infection with zones of necrotic tissue extending beneath the lesions. The decay extended progressively in diameter during cold storage, showing incidences of infection which exceeded 70% after 90 and 120 days' incubation in pears and apples, respectively. The fruit cultivar had no significant effect on the lesion diameter in wound-inoculated fruit, and no consistent differences in virulence were recorded among the isolates tested in these trials (data not reported). Some differences in disease symptomatology appeared when conidiomata became visible on fruit after longer periods of incubation (Table 3). All isolates of PvM-I formed superficial conidiomata which emerged on fruit skin after some months in cold storage (Table 3 and Figure 5), while the isolates belonging to PvM-II formed conidiomata in deeper fruit tissues (Table 3 and Figure 6), which remained below the

skin for a more extended period. Among the isolates of PvM-I, the majority (F1, F4, PFUTalca27, RS1, RS2 and ZOF3, 55%) were only able to form conidiomata on the skin of wound-inoculated fruit, while other isolates also produced some conidiomata within the outer part (about 15 mm below the skin) of the hypanthium (flesh) of all apple cultivars (F8, F19 and PNV1, 27%) or within the outer flesh of the cultivars Golden Delicious and Cripps Pink (F60 and RS4, 18%). Among the isolates of PvM-I, F4, RS1 and ZOF3 showed the earlier eruption of conidiomata on skin both on pear and apple (90 dpi in pears, 120 dpi in Golden Delicious and Cripps Pink apples), while RS2 showed the latest eruption of conidiomata (120 dpi in pears and 210–250 dpi in apples). The conidiomata of PvM-I were initially located below the cuticle, but they erupted on the fruit surface as they matured (Table 3 and Figure 5). They were medium-large, white-cream (rarely brown) and developed white hyphae with the advance of the decay. Among the isolates of PvM-I, F19 formed the smallest conidiomata (Figure S4). The first formation of conidiomata of PvM-II (F13, F14A and ID02) were observed 90 dpi in pear and 120 dpi in apple as small protuberances pushing on the surface of the lesion from the subepidermal tissue, sometimes displayed in rings around the centre of inoculation, and emerged later on the fruit skin (Table 3 and Figure 6). In addition, many conidiomata were formed by the isolates of PvM-II within the hypanthium (flesh) and mesocarp (core) of Golden Delicious (Figure 6j,k) and Cripps Pink apples (Figure 6n,q,s) and the outer part of the hypanthium of Kaiser pears (Figure 6c) and Granny Smith apples (Figure 6u). Some types of symptoms were specific to certain isolates of *P. vagabunda*. Zoned decays having a large lighter centre were formed in Kaiser pear infected with F4, F8, F19, PFUTalca27, PNV1, RS2 and ZOF3; yellowish lesions were observed in Cripps Pink apples infected with PNV1; and a pale halo surrounded the lesions in apples infected with the isolates F4, F8, F19, F60, PNV1, RS1, ZOF3. Other differences related to the amount of sporulation and the size of conidia formed in the different hosts. Most isolates of *P.*

*vagabunda* sporulated more abundantly on Cripps Pink and Golden Delicious apples, and, in particular, the isolates F60, PFUTalca27, PNV1, RS2 and RS4 of PvM-I showed only sporadic sporulation on Kaiser pears and/or Granny Smith apples. Overall, RS2 showed the latest sporulation and the least amount of conidia, especially on Granny Smith (Table 3). All isolates of *P. vagabunda* formed macroconidia (from 21 to 30  $\mu\text{m}$  long, straight or allantoid, rounded at both ends) on the surface of Cripps Pink and Golden Delicious apples 180 dpi, while some isolates of PvM-I formed shorter conidia on Granny Smith apple and Kaiser pear (PFUTalca27 and RS2) or on Kaiser pear (F8, F19, F60, PNV1 and RS4) (Figure S4). Conversely, the isolates of PvM-II (F10, F13, F14A and ID02) formed masses of macroconidia on all hosts tested.

The isolate NK1 of *N. kienholzii* usually developed aerial mycelium around the wound used for the inoculation and caused the formation of a pale halo around the lesion of decay (Figure 7). This isolate mainly formed superficial conidiomata, medium-large in size and white-cream in colour, which erupted on the fruit surface 90 dpi in Kaiser pear, 120 dpi in Golden Delicious and Cripps Pink apples and 180 dpi in Granny Smith apples; the isolate also formed some conidiomata within the outer layers of flesh. Peculiar traits of NK1 were the formation of sporodochial conidiomata on older lesions and the production of short (<12  $\mu\text{m}$  long on average) and straight conidia, slightly pointed, and often showing guttules.

The necrotic tissue of pear remained firmer and paler than that formed in apple, and sometimes included cavities at the margin of the decay (Figures 5–7). Apples and pears infected with *P. vagabunda* and *N. kienholzii* lost water progressively, becoming sunken and shrivelled; the rotten area covered the whole fruit after about 6-9 months' incubation in pears and 9–12 months' incubation in apples, and the formation of mummies occurred after 12–18 months of cold storage. The fruit infected with isolates of PvM-II were usually subsequently invaded by *Penicillium* spp., which sporulated abundantly and caused watery maceration in

advanced decays, while fruit infected with isolates of PvM-I or *N. kienholzii* were less susceptible to such secondary infections. Interestingly, hyaline or pigmented mycelial cords were recorded on all cultivars infected with *P. vagabunda* and *N. kienholzii* (Table 3 and Figures 5–7), but with more abundance on Cripps Pink apples. The formation of these hyphal aggregates was initially noticed 120–180 dpi as short filaments (few mm long) emerging from lenticels on apparently intact skin (without large breaks), and later also from conidiomata and sometimes flesh tissue (Figure S5 and Figure 6). They elongated during cold storage, becoming visible to the naked eye on the fruit surface and sometimes the stem in advanced decays (Figure 5, Figures S3 and S4). These mycelial cords were formed by fusion or coiling of several hyphae, and sometimes showed the growth of tendril hyphae on their surface.

### 3.5.2 Unwounded apples and pears

To simulate better the natural conditions of infection, unwounded fruit (of the same cultivars used for wound inoculation) were inoculated with the isolates F1, F8, ID02 of *P. vagabunda* and the isolate NK1 of *N. kienholzii*. The first manifestation of bull's eye rot symptoms was recorded 60 dpi on Kaiser pear, 90 dpi on Cripps Pink and Golden Delicious apples and 120 dpi on Granny Smith apples and consisted of one or numerous circular brown lesions on a single fruit. The incidence and severity of the disease (including number of lesions per fruit, extension of the diameter of lesions on fruit surfaces and rot beneath in flesh) increased with the progression of cold storage. After 120 days' incubation, the cultivars Kaiser, Golden Delicious and Cripps Pink showed greater susceptibility to the disease (incidence of infection ranging from 50% to 100% in Kaiser pears, from 35% to 60% in Golden Delicious and from 26% to 90% in Cripps Pink apples, depending on isolate) than the cultivar Granny Smith (incidence of disease  $\leq 30\%$ ; Figure 8). In particular, the infections by NK1 of *N. kienholzii* and F1 of *P. vagabunda* remained symptomless in Granny Smith apples at 120 dpi, and

caused only low incidence of disease in this cultivar 180 dpi (5% and 15% by NK1 and F1, respectively). The formation of cavities was often recorded in the internal rotted tissue of pear infected with the isolates F1 and F8 of the PvM-I and NK1 of *N. kienholzii* (Figure 9a–d). These isolates formed only superficial conidiomata on unwounded fruit, which erupted on the skin 180 dpi, while the isolate ID02 of PvM-II formed conidiomata which remained longer within the subepidermal tissue of fruit and also conidiomata within the flesh and the core of Cripps Pink (Figure 9e) and Golden Delicious apples. Besides infections on the sides of the fruit (Figure 9f–i), the isolates F8 and ID02 of *P. vagabunda* and NK1 of *N. kienholzii* frequently caused stem-end infections on apple (Figure 9j) and formed conidiomata on the stem of advanced decays (Figure 9k). The isolate NK1 of *N. kienholzii* showed the most abundant development of aerial mycelium, especially on mummies of Cripps Pink apple (Figure 9l). Mycelial cords of *N. kienholzii* and *P. vagabunda* were recorded on fruit skin and stem, and more abundantly on fruit infected with NK1 (Figure 9m) and F8 (Figure 9n,o); they were also observed within the flesh of Cripps Pink apples infected with the isolate ID02 of *P. vagabunda* (Figure 9p).

## 4 Discussion

This study emphasized the prevalence of *P. vagabunda* as causal agent of apple bull's eye rot in Italy and Chile and detected *N. kienholzii* as a less frequent cause of this disease in Italy. The morphological characterization of a wide number of isolates over an extended period of incubation showed a wide phenotypic variability within *P. vagabunda* and provided a description and illustration of further differences between the main morphotypes of the pathogen (Cameldi et al., 2017). Specific in vitro traits of PvM-I (the most frequent morphotype in the examined population) were the production of microconidia arising from

free mycelium, the late eruption of conidiomata on mature colonies and the formation of mycelial cords, especially on TA (the medium which favoured both sporulation and mycelial growth). Conversely, the isolates of PvM-II showed less marked development of aerial mycelium, but earlier formation of masses of macroconidia within conidiomata immersed in agar media. Four morphological subclades were delineated within PvM-I, and most of the Chilean isolates were grouped in a specific subclade (PvM-ID), characterized by conidiomata deeply immersed in agar media. In agreement with Amaral Carneiro et al. (2022), *N. kienholzii* showed slower growth than *P. vagabunda* on TA but grew faster on PDA. However, similarities were recorded between PvM-I and *N. kienholzii* NK1 concerning the hyphal organization, abundance of exudates and site of formation of conidia. Remarkably, the formation of hyphal structures never described before (highly branched hyphae and mycelial cords) was observed in many isolates of PvM-I and NK1 grown on TA. Fungi have been shown to vary their hyphal organization during growth in different conditions (Harris, 2008; Moore et al., 2004; Yafetto, 2018), but the role of the new hyphal structures recorded in *P. vagabunda* and *N. kienholzii* is unknown. Certainly, hyphal branching increases the surface area of mycelium. This phenomenon might favour fungi in essential activities, such as enhancing the assimilation of nutrients, the sensing of local environment, and the dispersal of conidia. Moreover, the fusion of hyphae in mycelial cords may allow the exchange of signals and nutrients within the colony. Drops of exudates were recorded on the colony surface of all isolates tested, but more abundantly in *N. kienholzii* and PvM-I. The phenomenon of guttation usually involves release of water and bioactive compounds useful for maintaining a constant growth of aerial hyphae and the formation of fungal structures (Krain & Siupka, 2021); this suggests that the exudates of *P. vagabunda* and *N. kienholzii* may favour the growth of these pathogens. All isolates of *P. vagabunda* and *N. kienholzii* assayed in the present study sporulated more profusely on TA (a nutrient-rich medium) than on PDA (a standard medium)

(Neri et al., 2019). However, the Chilean isolates of *P. vagabunda* sporulated less on TA than the majority of the Italian isolates. Disparate results have been reported in the literature regarding the capability of *P. vagabunda* to form conidia *in vitro*, ranging from inability to sporulate (Romero et al., 2018; Rooney-Latham & Soriano, 2016; Soto-Alvear et al., 2013; Trouillas et al., 2019), ability to sporulate only on specific substrates (Bompeix, 1966; Cameldi et al., 2017; Everett et al., 2017; Neri et al., 2009; Spotts et al., 2009), up to sporulation even on PDA (Rooney-Latham et al., 2013). These results suggest that the nutritional requirements necessary to promote sporulation probably vary within *P. vagabunda*, and the geographic area of collection and/or the host of origin might also influence the ability of this pathogen to sporulate *in vitro*.

In our study, we observed the growth of *P. vagabunda* and *N. kienholzii* on different hosts kept in cold storage until the formation of mummies. Important intra- and inter-species differences were detected in the location of conidiomata within the host: this was more superficial (mainly the skin) in fruit inoculated with PvM I and *N. kienholzii*, and deeper (skin and flesh, up to core in Cripps Pink and Golden Delicious apples) in fruit inoculated with PvM-II. Fungi can use light as a source of information about their environment and those causing bull's eye rot possess negative phototropism (Olsson, 1965). These pathogens probably find an optimal habitat within fruit tissues, where they remain unnoticed for some months before switching to a necrotrophic lifestyle (Neri et al., 2019). The ability of PvM-II isolates to live longer below the fruit skin and to form many conidiomata within fruit flesh suggests that the protection of fruit against this morphotype might require measures able to reach into and kill the pathogen in tissues far from the site of penetration. Moreover, the Italian isolate NK1 of *N. kienholzii* formed shorter conidia than those formed by *P. vagabunda* *in vivo* and produced profuse aerial mycelium on its fruit host, in agreement with the description reported for the USA isolates of this pathogen (Spotts et al., 2009). As found

on olive (Romero et al., 2018), fruit wounding favoured the penetration of *P. vagabunda* and *N. kienholzii* into host tissues, allowing the manifestation of severe lesions of disease, including in Granny Smith apples, which are known to show low susceptibility to bull's eye rot. In contrast, inoculating unwounded fruit demonstrated different degrees of susceptibility to the disease among the cultivars tested, with Granny Smith apples the least susceptible, in agreement with other reports (Di Francesco et al., 2019; Gariepy et al., 2005; Neri et al., 2009; Soto-Alvear et al., 2013). This suggests that the intact skin of Granny Smith apple may provide a more effective physical defence barrier against the invasion by *P. vagabunda* and *N. kienholzii* than the other cultivars tested. Besides the incidence of infection, the fruit cultivar also influenced the ability of the pathogen to sporulate. Interestingly, only the cultivars Cripps Pink and Golden Delicious allowed a steady formation of macroconidia by all isolates of *P. vagabunda* tested, and Cripps Pink allowed the most profuse formation of mycelial cords by *P. vagabunda* and *N. kienholzii*. Changes in the volatile blend emitted by Cripps Pink apples have been found to stimulate *P. vagabunda* growth during fruit storage (Neri et al., 2019), but other characteristics of the host, such as the nutritional factors and textural properties, may also favour the development of bull's eye rot in this cultivar. The pathogenicity tests on unwounded fruit also revealed varying degrees of virulence among the isolates. The high production of xylanase and cellulase recorded in the *P. vagabunda* isolate ID02 (Di Francesco et al., 2019) may have caused the high virulence we observed for this isolate and also the greater maceration of host tissue, which favoured the establishment of secondary infection by *Penicillium* spp. in fruit infected with this isolate.

In this work, we assessed whether the high degree of variability observed within *P. vagabunda* could be investigated further by sequence analysis of (i) new regions of genes routinely employed for *Phlyctema* and *Neofabraea* spp. characterization and phylogenetic analysis (*TUB2*), and (ii) new genomic regions determined in this work for the first time

(*ACT1*). Three out of the four selected genes showed at least two and up to a maximum of 17 SNPs in their sequences, confirming *TUB2* as the best marker gene to assess both inter- and intraspecific genetic distances. In contrast to Amaral Carneiro et al. (2022), we did not find any nucleotide differences among the *EF-1 $\alpha$*  sequences of *P. vagabunda*, even from different geographic origins (Chile and Italy); this may have been due to the short length of the fragment amplified in our study. Combining sequencing results from the four genomic regions, the 50 *P. vagabunda* isolates could be divided into 12 sequence types, three of which were specific to a distinct geographic region of the Southern hemisphere. The phylogenetic analysis grouped the Chilean isolates into two specific phylogroups (III and IV) distinct from those containing the Italian isolates. This suggests that part of the genetic diversity recorded within *P. vagabunda* is related to geographic origin, as also observed in a study of *P. vagabunda* on olive (Romero et al., 2018). Most Italian isolates clustered in phylogroups I and II, while the Italian isolates within the phylogroup V and VI represented three sequence types less frequent among the isolates of *P. vagabunda* tested. This could be explained by a low natural frequency of certain mutations, as well as by a different geographic origin associated with the transport of infected plant material or fungal inoculum. With the exception of phylogroups IV and V, which contained few isolates, the remaining phylogroups included isolates showing different morphological traits in vitro, indicating a lack of correspondence between phylogroups and morphotypes. Nevertheless, the phylogeny results were consistent with some aspects of the pathogen's biology. In particular, PvM-II isolates, which formed conidiomata immersed in agar media and deep in fruit tissue, were present only in phylogroup I, while PvM-IA isolates, which formed more superficial conidiomata, were included only in the phylogroups II and VI. The presence of other phenotypic traits in the same phylogenetic clusters suggests that the mutations found in the three genomic regions examined in our study are not sufficient to explain the diversity recorded in *P. vagabunda*,

and that a search for new sequence differences could provide better discrimination within phylogenetic groups. Overall, our results allowed us to explore further the intraspecific diversity of *P. vagabunda* isolates. In this study, they were distributed into six phylogenetic groups, which showed some degree of correlation with the geographic distribution of the isolates and their types of conidiomata and conidia formed in vitro and in vivo. More information could be obtained by expanding isolate collection to other geographic regions and/or searching for new genomic regions with an even higher level of genetic variability.

The biological cycle of *P. vagabunda* is poorly understood. Our assays carried out in an apple orchard demonstrated that rainwater is involved in the dispersal of *P. vagabunda* and that propagules of both morphotypes of this pathogen are present in rainwater collected from September to October in Italy. Conversely, *P. vagabunda* was not detected from rainwater collected from June to August, indicating that the inoculum of this pathogen is probably low during spring and summer, but increases towards autumn. Similar trends in pathogen concentration were recorded in studies on Cripps Pink fruit (Den Breeyen et al., 2020) and necrotic tissues of pear and apple (Köhl et al., 2018). In addition to fungal conidia, mycelial cords were also present in rainwater we collected from September to October. Such mycelial cords was also observed on fruit artificially inoculated with *P. vagabunda* and *N. kienholzii*, before the eruption of conidiomata on the fruit surface. The formation of mycelial cords by these pathogens may enable them to explore the environment and search for new nutrients, once the resources essential for growth have been depleted from the necrotized tissues (Harris, 2008; Yafetto, 2018). Mycelial cords of other fungi have been demonstrated to serve as repository organs for absorbed nutrients, able to give rise to new mycelia when they encounter favourable conditions of growth. Therefore, the mycelial cords of *P. vagabunda* and *N. kienholzii* may be potential sources of inoculum, contributing to the propagation of bull's eye rot from the mummies in the orchard (Köhl et al., 2018).

In conclusion, our study provided a description and illustration of *P. vagabunda* and *N. kienholzii* isolates, combining morphological and pathological data with molecular analysis of genomic regions routinely employed for the characterization of fungi. The results demonstrated the existence of morphological and genetic variability within *P. vagabunda* populations from different sources and geographic origins. Information on the dispersal of inoculum in the orchard provided new insights into the timing and mode of fruit infection, which are important for understanding the epidemiology of bull's eye rot and essential for effective control strategies.

## Acknowledgements

This research was partially supported by the project 'Innovative Models and Technologies for the quality and safety of Fruit and Vegetable products (M.I.T.O)' funded by Ministero dello Sviluppo Economico, 'HORIZON2020' European Regional Development Fund: PON I&C 2014-2020 - project no. F/050081/01-03/X32 - decree of funding 4 August 2016 prot. no. 0004763. CUP: B88I17000540008.

## Data availability statement

The data that support the findings of this study are available from the corresponding author upon reasonable request.

## References

Amaral Carneiro, G.A., Walcher, M., Storti, A. & Baric, S. (2022) Phylogenetic diversity and

phenotypic characterization of *Phyctema vagabunda* (syn. *Neofabraea alba*) and *Neofabraea kienholzii* causing bull's eye rot of apple in northern Italy. *Plant Disease* 106, 451–463.

Bompeix, G. (1966) *Contribution a l'étude de la maladie des taches lenticellaires des pommes "Golden Delicious" en France*. Faculte des Sciences de Rennes Collège Scientifique Universitaire de Brest. DES thesis.

Cameldi, I., Neri, F., Menghini, M., Pirondi, A., Nanni, I.M., Collina, M. et al. (2017) Characterization of *Neofabraea vagabunda* isolates causing apple bull's eye rot in Italy (Emilia-Romagna region). *Plant Pathology*, 66, 1432–1444.

Cao, D., Li, X., Cao, J. & Wang, W. (2013) PCR detection of the three *Neofabraea* pathogenic species responsible for apple bull's eye rot. *Advances in Microbiology*, 3, 61–64.

Chen, C., Verkley, G.J.M., Sun, G., Groenewald, J.Z. & Crous, P.W. (2016). Redefining common endophytes and plant pathogens in *Neofabraea*, *Pezicula*, and related genera. *Fungal Biology* 120, 1291–1322.

Chernomor, O., von Haeseler, A. & Minh, B.Q. (2016) Terrace aware data structure for phylogenomic inference from supermatrices. *Systematic Biology*, 65, 997-1008.

Den Breeyen, A., Rochefort, J.R., Meitz-Hopkins, J. & Lennox, C.L. (2020) Preharvest detection and postharvest incidence of *Phlyctema vagabunda* on Cripps Pink apples in South Africa. *Plant Disease*, 104, 841–846.

Di Francesco, A., Cameldi, I., Neri, F., Barbanti, L., Folchi, A., Spadoni, A. et al. (2019) Effect of apple cultivars and storage periods on the virulence of *Neofabraea* spp. *Plant*

*Pathology*, 68, 1525–1532.

Doyle, J.J. & Doyle, J.L. (1987) A rapid DNA isolation procedure for small quantities of fresh leaf tissue. *Phytochemical Bulletin*, 19, 11–15.

Everett, K.R., Pushparajah, I.P.S., Fisher, B.M. & Wood, P.N. (2017) A simple method for conidial production and establishing latent infections of apples by *Phlyctema vagabunda* (syn: *Neofabraea alba*). *New Zealand Plant Protection*, 70, 106–111.

Gardes, M. & Bruns, T.D. (1993) ITS primers with enhanced specificity for basidiomycetes—application to identification of mycorrhizae and rusts. *Molecular Ecology*, 2, 113–118.

Garipey, T.D., Rahe, J.E., Lévesque, C.A., Spotts, R.A., Sugar, D.L. & Henriquez, J.L. (2005) *Neofabraea* species associated with bull's-eye rot and cankers of apple and pear in the Pacific Northwest. *Canadian Journal of Plant Pathology*, 27, 118–124.

Groenewald, J.Z., Nakashima, C., Nishikawa, J., Shin, H.D., Park, J.H., Jama, A.N. et al. (2013) Species concepts in *Cercospora*: spotting the weeds among the roses. *Studies in Mycology*, 75, 115–170.

Harris, S.D. (2008) Branching of fungal hyphae: regulation, mechanisms and comparison with other branching systems. *Mycologia*, 100, 823–832.

Henriquez, J.L., Sugar, D. & Spotts, R.A. (2004) Etiology of bull's eye rot of pear caused by *Neofabraea* spp. in Oregon, Washington, and California. *Plant Disease*, 88, 1134–1138.

Johnston, P., Seifert, K.A., Stone, J., Rossman, A.Y. & Marvanová, L. (2014) Recommendations on generic names competing for use in Leotiomycetes

(Ascomycota). *IMA Fungus*, 5, 91–120.

de Jong, S.N., Lévesque, C.E., Verkley, G.J.M., Abeln, E.C.A., Rahe, J.E. & Braun, P.G.

(2001) Phylogenetic relationships among *Neofabraea* species causing tree cankers and bull's-eye-rot of apple based on DNA sequencing of ITS nuclear rDNA, mitochondrial rDNA, and the  $\beta$ -tubulin gene. *Mycological Research*, 105, 658–669.

Kalyaanamoorthy, S., Minh, B.Q., Wong, T.K.F., von Haeseler, A. & Jermini, L.S. (2017)

ModelFinder: Fast model selection for accurate phylogenetic estimates. *Nature Methods*, 14, 587–589.

Köhl, J., Wencker, M., Groenenboom-de Haas, B.H., Anbergen, R., Goossen-van de Geijn,

H.M., Lombaers-van der Plas, C.H. et al. (2018). Dynamics of post-harvest pathogens *Neofabraea* spp. and *Cadophora* spp. in plant residues in Dutch apple and pear orchards. *Plant Pathology* 67, 1264–1277.

Krain, A. & Siupka, P. (2021) Fungal guttation, a source of bioactive compounds, and its ecological role-a review. *Biomolecules*, 11, 1270.

Kumar, S., Stecher, G., Li, M., Knyaz, C. & Tamura, K. (2018) MEGA X: Molecular

evolutionary genetics analysis across computing platforms. *Molecular Biology and Evolution*, 35, 1547–1549.

Li, W.J., McKenzie, E.H.C., Liu, J.K.J., Bhat, D.J., Dai, D.Q., Camporesi, E. et al. (2020)

Taxonomy and phylogeny of hyaline-spored coelomycetes. *Fungal Diversity*, 100, 279–801.

Michalecka, M., Bryk, H., Poniatowska, A. & Pulawska, J. (2016) Identification of

*Neofabraea* species causing bull's eye rot of apple in Poland and their direct detection

- in apple fruit using multiplex PCR. *Plant Pathology*, 65, 643–654.
- Moore, D., McNulty, L.J. & Meskauskas A (2004) Branching in fungal hyphae and fungal tissues: growing mycelia in a desktop computer. In: Davies, J. (Ed.) *Branching morphogenesis*. Molecular Biology Intelligence Unit. Springer-Verlag, pp. 75–90.
- Neri, F., Cappellin, L., Aprea, E., Biasioli, F., Gasperi, F., Spadoni, A. et al. (2019) Interplay of apple volatile organic compounds with *Neofabraea vagabunda* and other postharvest pathogens. *Plant Pathology*, 68, 1508–1524.
- Neri, F., Mari, M., Brigati, S. & Bertolini, P. (2009) Control of *Neofabraea alba* by plant volatile compounds and hot water. *Postharvest Biology and Technology*, 51, 425–430.
- Nguyen, L.T., Schmidt, H.A., von Haeseler, A. & Minh, B.Q. (2015) IQ-TREE: A fast and effective stochastic algorithm for estimating maximum likelihood phylogenies. *Molecular Biology and Evolution*, 32, 268–274.
- Olsson, K. (1965) A study of the biology of *Gloeosporium album* and *G. perennans* on apples. *Meddelanden Statens Växtskyddsanstalt*, 13, 189–259.
- Rehner, S.A. & Buckley, E.P. (2005) A *Beauveria* phylogeny inferred from nuclear ITS and EF1- $\alpha$  sequences: evidence for cryptic diversification and links to *Cordyceps* teleomorphs. *Mycologia*, 97, 84–98.
- Romero, J., Raya, M.C., Roca, L.F., Agusti-Brisach, C., Moral, J. & Trapero, A. (2018) Phenotypic, molecular and pathogenic characterization of *Phlyctema vagabunda*, causal agent of olive leprosy. *Plant Pathology*, 67, 277–294.
- Rooney-Latham, S., Gallegos, L.L., Vossen, P.M. & Gubler, W.D. (2013) First report of *Neofabraea alba* causing fruit spot on olive in North America. *Plant Disease*, 97, 1384.

- Rooney-Latham, S. & Soriano, M.C. (2016) First report of *Neofabraea alba* causing canker dieback of apple in California. *Plant Disease*, 100, 1011.
- Soto-Alvear, S., Lolas, M., Rosales, I.M., Chávez, E.R. & Latorre, B.A. (2013) Characterization of the bull's eye rot of apple in Chile. *Plant Disease*, 97, 485–490.
- Spotts, R.A., Seifert, K.A., Wallis, K.M., Sugar, D., Xiao, C.L., Serdani, M. et al. (2009) Description of *Cryptosporiopsis kienholzii* and species profiles of *Neofabraea* in major pome fruit growing districts in the Pacific Northwest USA. *Mycological Research*, 113, 1301–1311.
- Sutton, B.C. (1980) *The Coelomycetes Fungi Imperfecti with picnidia, acervuli and stromata*. Kew, UK: Commonwealth Mycological Institute.
- Trouillas, F.P., Nouri, M.T., Lawrenc, D.P., Moral, J., Travadon, R., Aegerter, B.J. et al. (2019) Identification and characterization of *Neofabraea kienholzii* and *Phlyctema vagabunda* causing leaf and shoot lesions of olive in California. *Plant Disease*, 103, 3018–3030.
- Verkley, G.J.M. (1999) A monograph of the genus *Pezicula* and its anamorphs. *Studies in Mycology* 44, 125–127.
- Woudenberg, J.H.C., Aveskamp, M.M., de Gruyter, J, Spiers, A.G. & Crous, P.W. (2009) Multiple *Didymella* teleomorphs are linked to the *Phoma clematidina* morphotype. *Persoonia*, 22, 56–62.
- Yafetto, L. (2018) The structure of mycelial cords and rhizomorph of fungi: a mini-review. *Mycosphere* 9, 984–998.

## Supporting information legends

**Figure S1** Diversity in disease symptoms of bull's eye rot observed in fruit collected for this study.

**Figure S2** Diversity in the morphological features of colonies (a–d) and patterns of growth (e) represented by some isolates of *Phlyctema vagabunda* and the isolate NK1 of *Neofabraea kienholzii* grown on tomato agar (a, d) and potato dextrose agar (b, c, front and reverse, respectively) after 30 (a–c) and 60 days' incubation (d) at 15°C.

**Figure S3** Bull's eye rot symptoms in pears and apples wound-infected with the isolate F19 (morphotype I) of *Phlyctema vagabunda*. (a–d) Kaiser pear, (e–g) Golden Delicious, (h–m) Cripps Pink and (n–p) Granny Smith apples. Yellow and black arrows in l indicate a mycelial cord and conidiomata on fruit stem, respectively. Fruit were infected with conidial suspensions of the pathogen ( $10^4$  conidia/ml) and stored at 0°C.

**Figure S4** Development of mycelial cords of *Phlyctema vagabunda* on fruit surface. (a–k) Observation under stereomicroscope and (l–x) microscope. Fruit were infected with conidial suspensions of the pathogen ( $10^4$  conidia/ml) and stored at 0°C.

**Table S1** Main morphological features of *Phlyctema vagabunda* and *Neofabraea kienholzii* isolates grown on tomato agar.

**Table S2** Main morphological features of *Phlyctema vagabunda* and *Neofabraea kienholzii* isolates grown on potato dextrose agar.

**Table S3** Correspondence between *Phlyctema vagabunda* phylogroups and morphotypes on tomato agar (TA) and potato dextrose agar (PDA).

## Figure legends

**Figure 1** Main features characterizing the growth of morphotype I and II of *Phlyctema vagabunda* (PvM-I and PvM-II) on tomato agar. (a–z) PvM-I; (a1–a6) PvM-II; (a–d) drops of hyaline (a and b) and pigmented (c and d) exudates on aerial hyphae; (e–h) highly branched hyphae; (i–m) PvM-I conidia (i) formed from linear (j) and branched hyphae (k–m); (n–t) black and pink mycelial cords on the surface of mature colonies; (u) PvM-I conidioma visible from washing of 30-day-old colonies; (v–y) PvM-I conidiomata (emerged or semi-immersed) on the surface of 60-day-old colonies, usually covered by exudates (v, w); (z) conidiomata formed by PvM-ID deeply immersed in agar medium, visible after the removal of aerial mycelium; (a1–a4) PvM-II conidiomata immersed in agar medium in 60-day-old colonies; (a5, a6) masses of conidia formed by PvM-II (a5) and released in mucilaginous drops on the agar surface (a6). Scale bar in micrographs = 100  $\mu\text{m}$ .

**Figure 2** Main features characterizing the growth of *Neofabraea kienholzii* (isolate NK1) on tomato agar. (a, b) Feathery fascicles of aerial hyphae; (c, d) drops of hyaline exudates on aerial hyphae; (e–l) mycelial cords recorded on 14-day-old colonies (e–j) and 60-day-old colonies (k, l); (m–p) conidia (m) arising from linear (n) and branched hyphae (o, p); (q, r) conidiomata immersed in agar medium in 40-day-old colonies, visible by the removal of aerial mycelium; (s–u) drops of mucilage (s, t) containing masses of conidia (u) in 75-day-old colonies; (v–x) emerged and semi-immersed conidiomata covered by exudates on 90-day-old colonies. Scale bar in micrographs = 100  $\mu\text{m}$ .

**Figure 3** Phylogenetic analysis of *Phlyctema vagabunda* and *Neofabraea kienholzii* isolates. The maximum-likelihood tree was obtained from the alignment of sequences from the ITS1, *EF-1 $\alpha$* , *TUB2* and *ACT1* genes. Bootstrap values reported at the nodes are from 5000 replicates. The tree was rooted on *N. kienholzii* sequences and visualized with a 70% cut-off

value. The phylogroups (I, II, III, IV, V and VI) are highlighted in different colours. The geographic origin is indicated by green and blue circles corresponding to Italian and Chilean isolates, respectively.

**Figure 4** Comparison of the 12 sequence variants obtained from the alignment of *Phlyctema vagabunda* ITS1, *EF-1 $\alpha$* , *TUB2* and *ACT1* concatenated sequences. Nucleotide differences are highlighted in yellow.

**Figure 5** Progression of bull's eye rot symptoms in pears and apples wound-inoculated with isolates of morphotype I of *Phlyctema vagabunda*. (a–h) Kaiser pear, (i–l) Golden Delicious, (m–s) Cripps Pink and (t–v) Granny Smith apples. (b) Crushing of fruit skin by the expansion of conidiomata initially formed within skin; (d, j, n) eruption of conidiomata on skin. (w) conidiogenous cells giving rise to conidia; (x) conidia. The black arrows indicate the formation of cavities in the internal rotted tissue of pear (e). The yellow arrows indicate mycelial cords formed on skin (g, h, q, r) and stem (k, s). The pictures are representative of the isolates F4, RS1 and ZOF3, which showed earlier eruption of conidiomata on fruit skin. Fruit were infected with conidial suspensions of the pathogen ( $10^4$  conidia/ml) and stored at 0°C.

**Figure 6** Progression of bull's eye rot symptoms in pears and apples wound-inoculated with isolates of morphotype II of *Phlyctema vagabunda*. (a–g) Kaiser pear, (h–k) Golden Delicious, (l–s) Cripps Pink and (t–v)– Granny Smith apples. (b) Subepidermal conidiomata; (e, i, m) appearance of subepidermal conidiomata on fruit surface; (k) conidiomata within flesh; (r, v) mummies showing eruption of the conidiomata on fruit surface and secondary infection of *Penicillium* spp.; (w, x) masses of conidia released on fruit surface. The white arrows indicate conidiomata formed within flesh and core (c, j, k, n, q, s, u). The black arrows indicate cavities formed in the internal rotted tissue of pear (c). The yellow arrows indicate

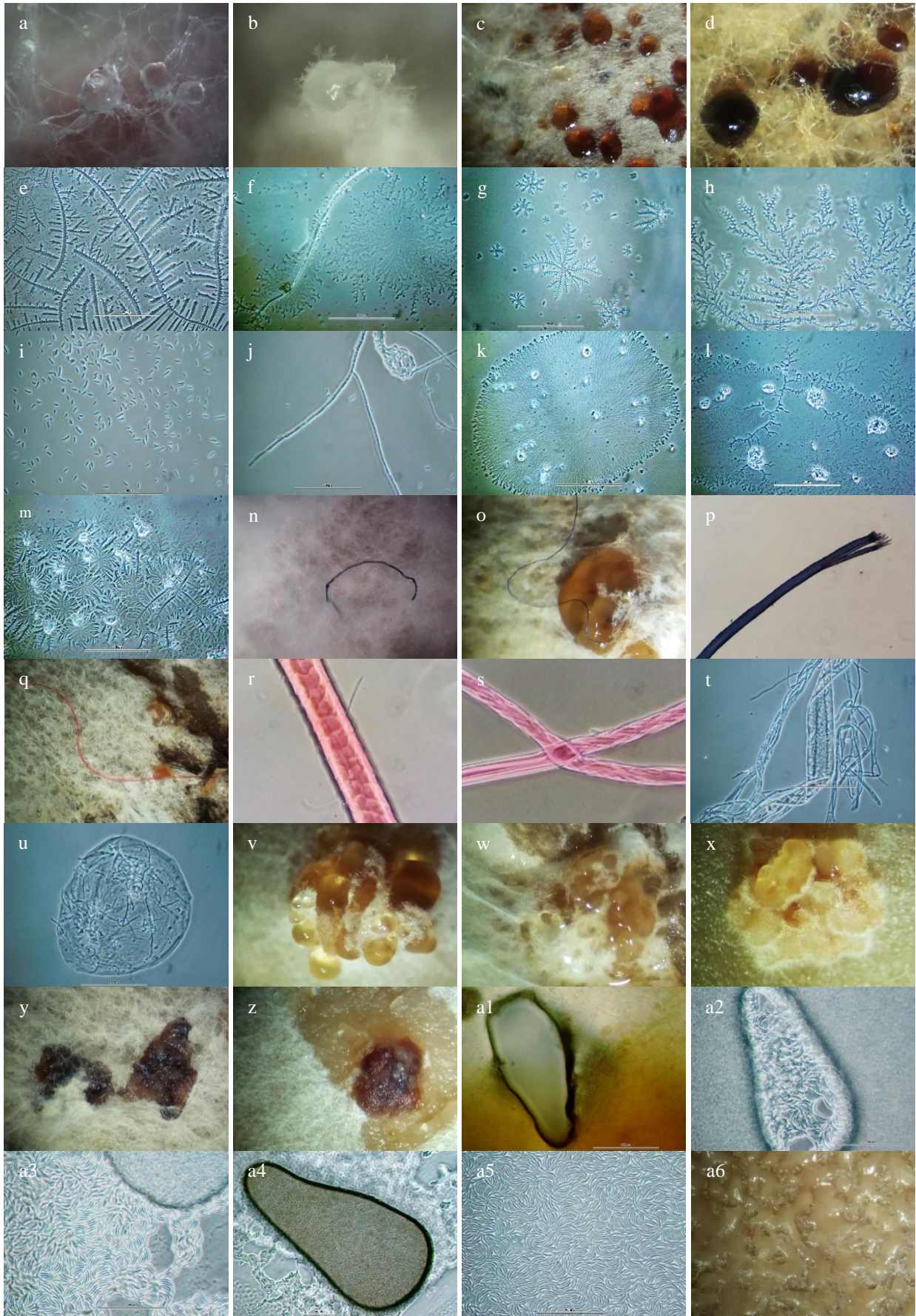
mycelial cords formed in flesh (c, g) and skin (p). Fruit were infected with conidial suspensions of the pathogen ( $10^4$  conidia/ml) and stored at 0°C.

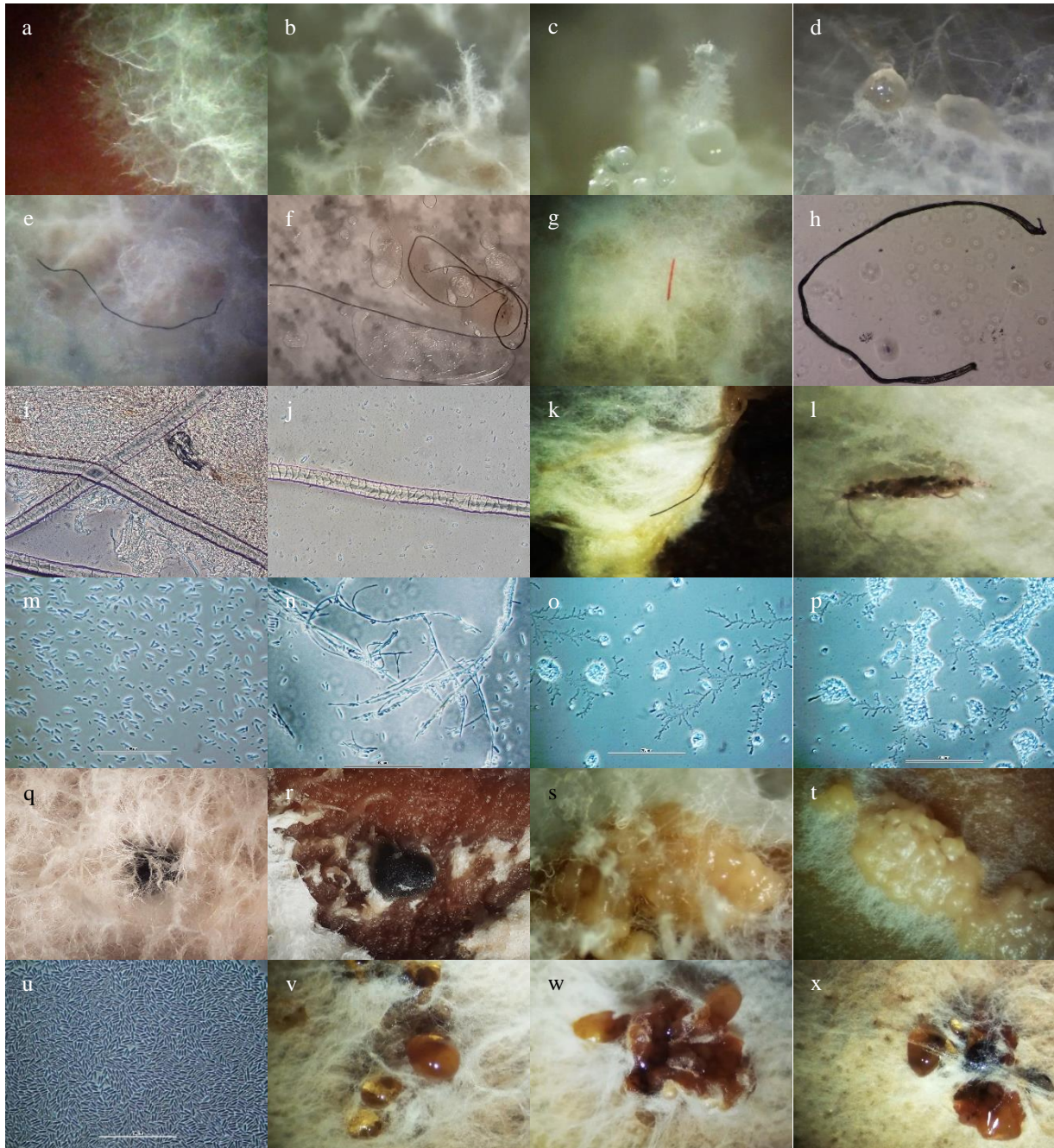
**Figure 7** Progression of bull's eye rot symptoms in pears and apples wound-inoculated with the isolate NK1 of *Neofabraea kienholzii*. (a–d) Kaiser pear, (e–i) Golden Delicious, (j–y) Cripps Pink and (z) Granny Smith apples. (b, h, i) eruption of conidiomata on fruit skin; (v–y) formation of sporodochial conidiomata on older lesions and mummies; (a1) conidiogenous cells giving rise to conidia; (a2) conidia. The white arrows indicate conidiomata formed on stem (n, s) and within the outer part of flesh (b, d, f). The black arrows indicate cavities formed in the internal rotted tissue of pear (d). The yellow arrows indicate mycelial cords formed on fruit lesions (l, t–v). Fruit were infected with conidial suspensions of the pathogen ( $10^4$  conidia/ml) and stored at 0°C.

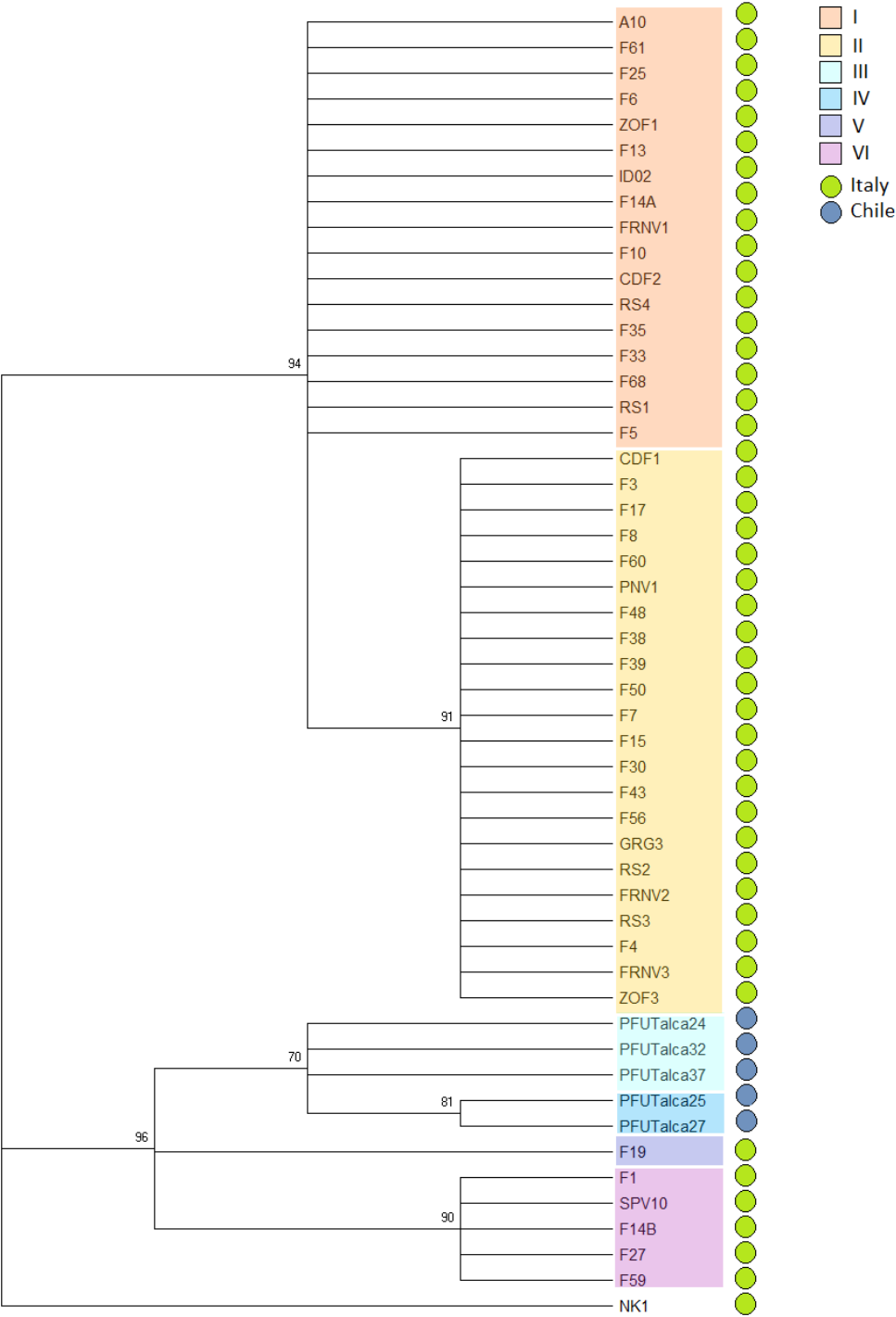
**Figure 8** Percentage of fruit with symptoms of bull's eye rot recorded 120 days postinoculation. Unwounded pears (cultivar Kaiser) and apples (cultivars Golden Delicious, Cripps Pink and Granny Smith) were sprayed with conidial suspensions ( $10^5$  conidia/ml) of *Phlyctema vagabunda* (isolates F1, F8 and ID02) and *Neofabraea kienholzii* (isolate NK1) and stored at 0°C. Within each isolate, columns with the same letter are not significantly different at  $p \leq 0.05$ , according to Tukey's test.

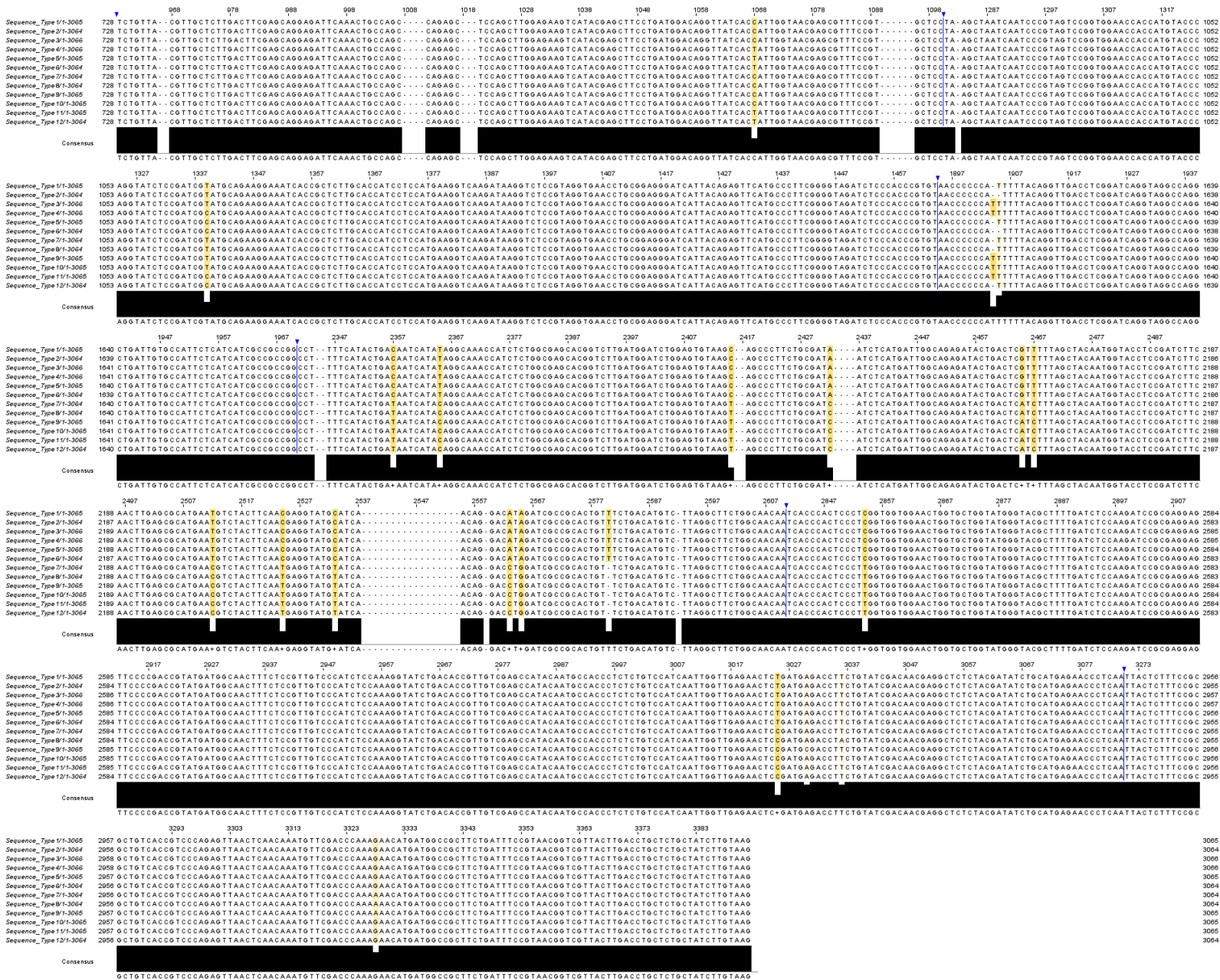
**Figure 9** Features recorded in unwounded pear (cultivar Kaiser) and apples (cultivars Golden Delicious, Granny Smith and Cripps Pink) infected with *Phlyctema vagabunda* (isolates F1, F8 and ID02) and *Neofabraea kienholzii* (isolate NK1). (a–d) formation of cavities in the internal rotted tissue of pear by the isolates F1, F8 and NK1; (e) formation of conidiomata within deep tissue of fruit by ID02; (f–i) formation of one or more decay lesions on the surfaces of fruit; (j) example of stem-end infection on apple by F8, ID02 and NK1; (k) example of formation of conidiomata on apple stem by F8, ID02 and NK1; (l) abundant

growth of aerial mycelium on fruit surface by NK1; (m–p) formation of mycelial cords on fruit skin (m, mycelium of NK1, n, conidioma of F8), stem (o, Granny Smith apple infected with F8) or flesh (p, Cripps Pink apple infected with ID02) in advanced decays. The white and yellow arrows indicate conidiomata and mycelial cords, respectively. Fruit were sprayed with conidial suspensions ( $10^5$  conidia/ml) of the pathogens and stored at 0°C.

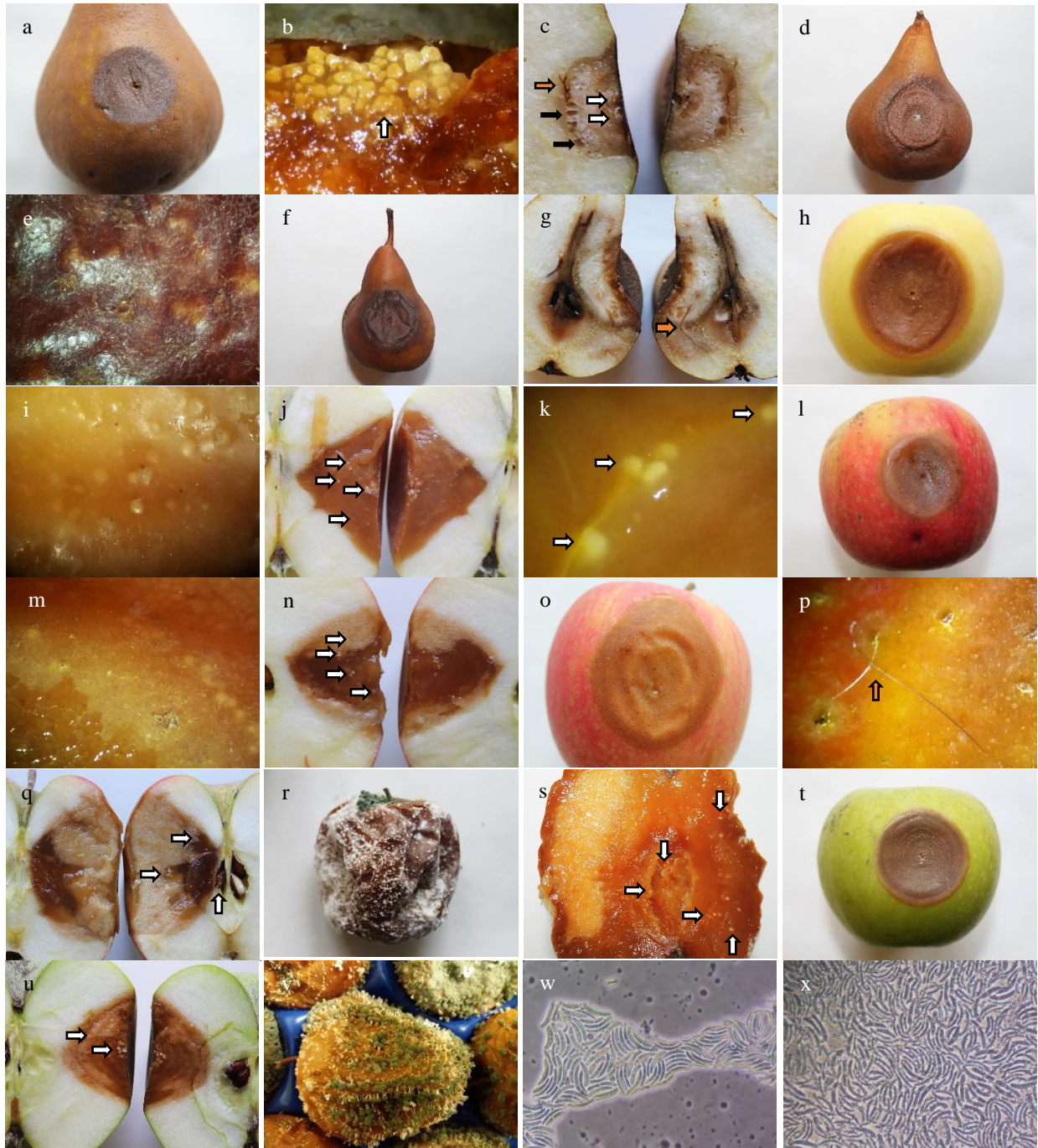


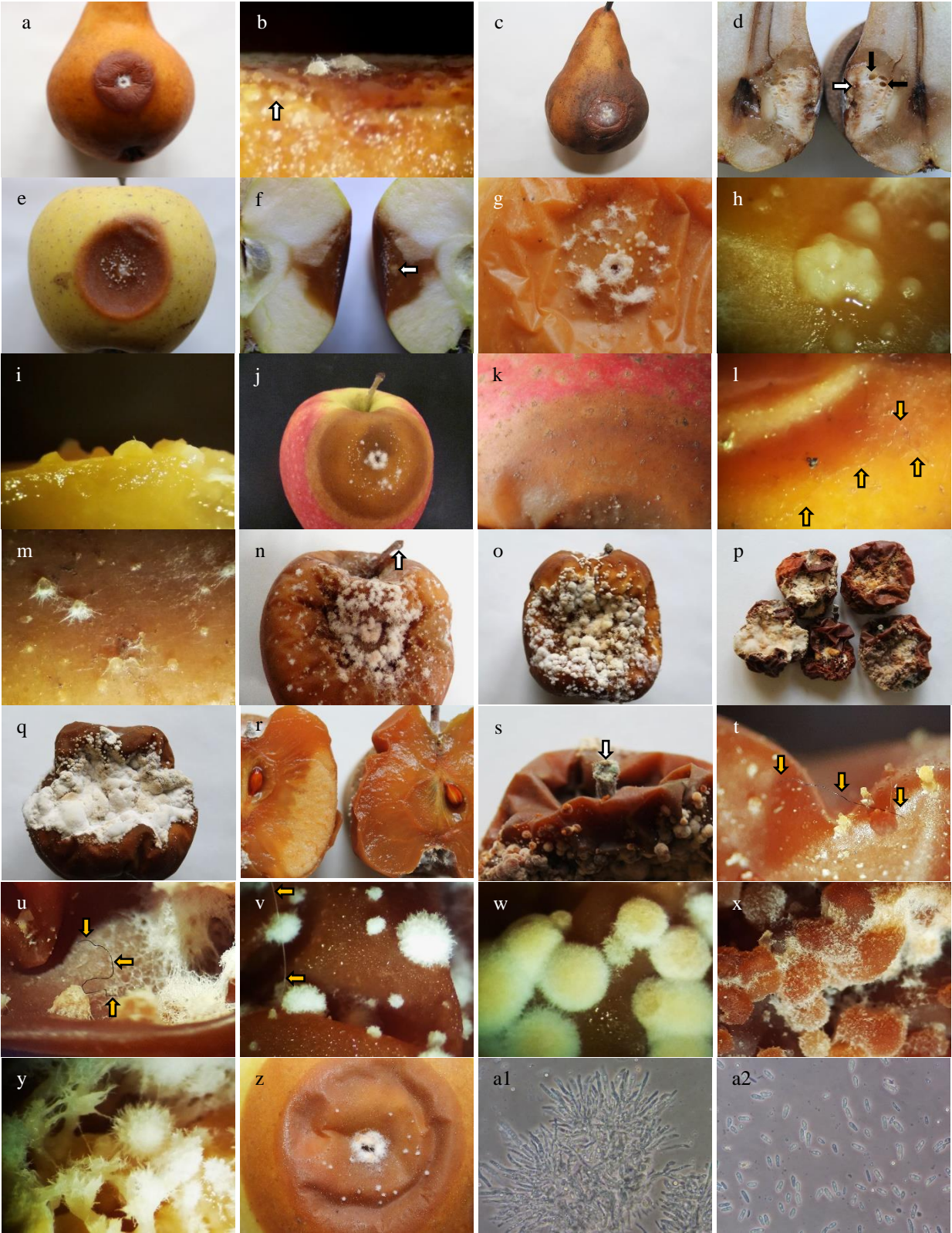


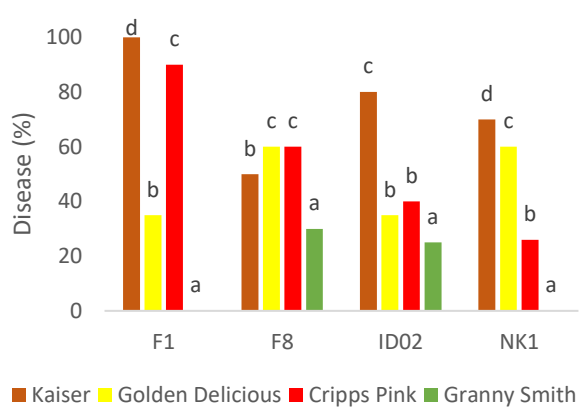












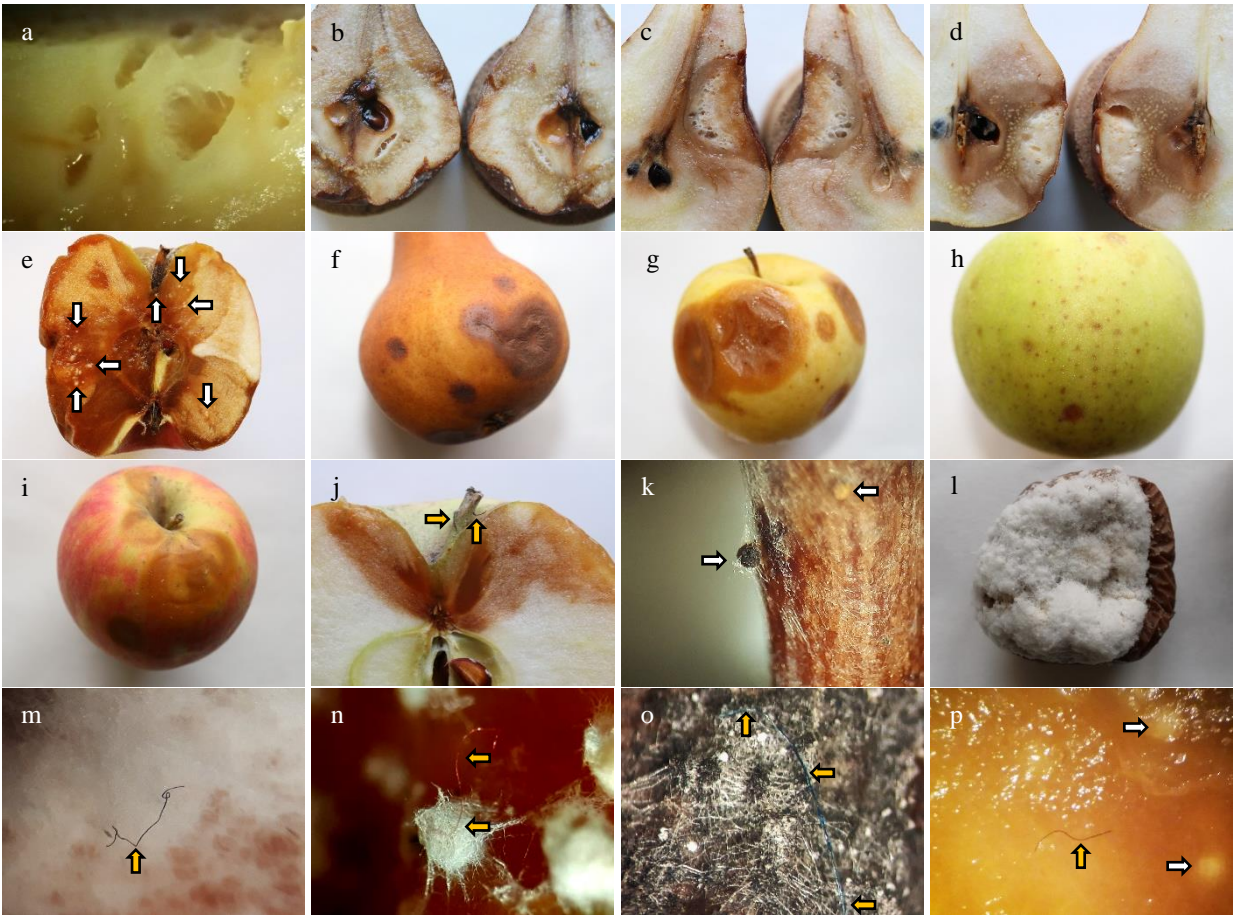


**Table 1** Fungal isolates characterized in this study and the partial sequences of ITS1, *TUB2*, *EF-1 $\alpha$*  and *ACT1* genes used to identify them as *Neofabraea kienholzii* (NK1) or *Phlyctema vagabunda* (all remaining isolates)

Isolate	Source				GenBank accession number				Sequence type
	Substrate	Cultivar	Year	Location	ITS1	<i>TUB2</i>	<i>EF-1<math>\alpha</math></i>	<i>ACT1</i>	
A10	Fruit	Cripps Pink	2014	Ravenna, Italy	OL638319	OL740329	OL740207	OL740304	1
CDF1	Fruit	Fuji	2015	Ferrara, Italy	OL638336	OL740346	OL740224	OL740265	4
CDF2	Fruit	Fuji	2015	Ferrara, Italy	OL638335	OL740345	OL740223	OL740266	1
F1	Fruit	Cripps Pink	2015	Bologna, Italy	OL638354	OL740364	OL740242	OL740306	11
F3	Fruit	Cripps Pink	2015	Bologna, Italy	OL638331	OL740341	OL740219	OL740307	4
F4	Fruit	Cripps Pink	2015	Bologna, Italy	OL638343	OL740353	OL740231	OL740272	5
F5	Fruit	Cripps Pink	2015	Bologna, Italy	OL638326	OL740336	OL740214	OL740273	3
F6	Fruit	Cripps Pink	2015	Bologna, Italy	OL638337	OL740347	OL740225	OL740274	1
F7	Fruit	Cripps Pink	2015	Bologna, Italy	OL638340	OL740350	OL740228	OL740275	4
F8	Fruit	Cripps Pink	2015	Bologna, Italy	OL638341	OL740351	OL740229	OL740276	4
F10	Fruit	Cripps Pink	2015	Bologna, Italy	OL638325	OL740335	OL740213	OL740277	1
F13	Fruit	Cripps Pink	2015	Bologna, Italy	OL638345	OL740355	OL740233	OL740278	1
F14A <sup>a</sup>	Fruit	Cripps Pink	2015	Bologna, Italy	OL638350	OL740360	OL740238	OL740279	1
F14B	Fruit	Cripps Pink	2015	Bologna, Italy	OL638327	OL740337	OL740215	OL740280	11
F15	Fruit	Cripps Pink	2015	Bologna, Italy	OL638342	OL740352	OL740230	OL740281	4
F17	Fruit	Cripps Pink	2015	Bologna, Italy	OL638323	OL740333	OL740211	OL740283	4
F19	Fruit	Cripps Pink	2015	Bologna, Italy	OL638324	OL740334	OL740212	OL740308	10

F25	Fruit	Cripps Pink	2017	Ravenna, Italy	OL638322	OL740332	OL740210	OL740286	1
F27	Fruit	Cripps Pink	2017	Ravenna, Italy	OL638320	OL740330	OL740208	OL740311	12
F30	Fruit	Cripps Pink	2017	Ravenna, Italy	OL638351	OL740361	OL740239	OL740287	5
F33	Fruit	Cripps Pink	2017	Ravenna, Italy	OL638329	OL740339	OL740217	OL740288	3
F35	Fruit	Cripps Pink	2017	Ravenna, Italy	OL638346	OL740356	OL740234	OL740289	3
F38	Fruit	Cripps Pink	2017	Ravenna, Italy	OL638352	OL740362	OL740240	OL740290	4
F39	Fruit	Cripps Pink	2017	Ravenna, Italy	OL638328	OL740338	OL740216	OL740291	4
F43	Fruit	Cripps Pink	2017	Ravenna, Italy	OL638369	OL740379	OL740257	OL740292	5
F48	Fruit	Cripps Pink	2017	Ravenna, Italy	OL638318	OL740328	OL740206	OL740312	4
F50	Fruit	Cripps Pink	2017	Ravenna, Italy	OL638330	OL740340	OL740218	OL740293	4
F56	Fruit	Cripps Pink	2018	Cesena, Italy	OL638363	OL740373	OL740252	OL740313	5
F59	Fruit	Cripps Pink	2018	Cesena, Italy	OL638366	OL740376	OL740255	OL740285	12
F60	Fruit	Cripps Pink	2018	Cesena, Italy	OL638333	OL740343	OL740221	OL740314	4
F61	Fruit	Cripps Pink	2019	Cesena, Italy	OL638316	OL740324	OL740203	OL740315	1
F68	Fruit	Cripps Pink	2019	Cesena, Italy	OL638317	OL740326	OL740205	OL740317	3
FRNV1	Rainwater	Cripps Pink	2015	Bologna, Italy	OL638355	OL740365	OL740243	OL740294	1
FRNV2	Rainwater	Cripps Pink	2015	Bologna, Italy	OL638338	OL740348	OL740226	OL740295	5
FRNV3	Rainwater	Cripps Pink	2015	Bologna, Italy	OL638334	OL740344	OL740222	OL740319	6
GRG3	Fruit	Cripps Pink	2016	Forli, Italy	OL638344	OL740354	OL740232	OL740297	5
ID02	Fruit	Cripps Pink	2014	Bologna, Italy	OL638353	OL740363	OL740241	OL740305	1
PFUTalca24	Fruit	Cripps Pink	2017	Angol, Chile	OL638314	OL740321	OL740198	OL740267	7

PFUTalca25	Fruit	Cripps Pink	2017	Longaví, Chile	MG969999	OL740320	OL740199	OL740268	9
PFUTalca27	Fruit	Cripps Pink	2017	Temuco, Chile	MG970000	OL740322	OL740200	OL740269	9
PFUTalca32	Fruit	Cripps Pink	2017	Coihueco, Chile	OL638315	OL740323	OL740201	OL740270	7
PFUTalca37	Fruit	Cripps Pink	2017	Mayol, Chile	MG969996	OL740327	OL740202	OL740271	8
PNV1	Fruit	Pinova	2016	Bologna, Italy	OL638321	OL740331	OL740209	OL740298	4
RS1	Fruit	Cripps Pink	2016	Ravenna, Italy	OL638347	OL740357	OL740235	OL740303	3
RS2	Fruit	Cripps Pink	2016	Ravenna, Italy	OL638349	OL740359	OL740237	OL740309	5
RS3	Fruit	Cripps Pink	2016	Ravenna, Italy	OL638360	OL740370	OL740249	OL740299	5
RS4	Fruit	Cripps Pink	2016	Ravenna, Italy	OL638362	OL740372	OL740251	OL740300	2
SPV10	Fruit	Cripps Pink	2014	Ravenna, Italy	OL638332	OL740342	OL740220	OL740301	11
ZOF1	Fruit	Cripps Pink	2016	Cesena, Italy	OL638367	OL740377	OL740256	OL740310	1
ZOF3	Fruit	Cripps Pink	2016	Cesena, Italy	OL638359	OL740369	OL740248	OL740302	6
NK1	Fruit	Cripps Pink	2017	Ravenna, Italy	OL662922	OL740380	OL740258	OL740259	–

---

<sup>a</sup>The isolates F14A and F14B originated from the same fruit.

**Table 2** Primers used in this study, their sequences and sources

Gene	Primer	Sequence (5′–3′)	Product size (bp)	Annealing temperature (°C)	Reference
ITS1	ITS1F	CTTGGTCATTTAGAGGAAGTAA	600	52	Gardes and Bruns (1993)
	ITS4	TCCTCCGCTTATTGATATGC			
<i>EF-1α</i>	EF1-983F	GCYCCYGGHCAYCGTGAYTTYAT	1000	50	Rehner and Buckley (2005)
	EF1-1567R	ACHGTRCCRATAACCACCRATCTT			
<i>TUB2</i>	Btub2Fd	GTBCACCTYCARACCGGYCARTG	c.1500	55	Woudenberg et al. (2009)
	Btub4Rd	CRGAYTGRCCRAARACRAAGTTGTC			
	tub2-F	CTTTCTCCGTTGTCCCATCC	554	57	Cao et al. (2013)
	tub2-R	GAACATTGCGCATCTGGTCC			
	Neo-TubFw	ACTGTATAGCTACAGATGCTG	c.1400	57	This study
	Neo-TubRev	TGGAGGACATCTTAAGACCACGAG			
<i>ACT1</i>	ACT1Fd	GCYGCBCTCGTYATYGACAATGG	1500	55	Groenewald et al. (2013)

---

ACT1Rd	CRTC GTACTCCTGCTTBGAGATCCAC			
ActNeoF	GATCTGTAGTTCGGGTATGTGC	c.1400	52	This study
ActNeoR	GCCAAGATGGAACCTCCAATCC			

---

**Table 3** Main traits recorded on pears and apples wound-inoculated with representative isolates of the *Phlyctema vagabunda* and *Neofabraea kienholzii* collection

Conidiomata																
Isolate	Position in fruit tissue				Time of appearance (dpi)				Conidia length (µm)				Mycelial cords on fruit skin			
	K	GD	CP	GS	K	GD	CP	GS	K	GD	CP	GS	K	GD	CP	GS
<i>P. vagabunda</i> (morphotype I)																
F1	Skin	Skin	Skin	Skin	120	120	120	180	21.5	27.2	27.7	7.0	Black	Black	Black	Black
F4	Skin	Skin	Skin	Skin	90	120	120	180	25	21.5	26.8	21.7	Black, hyaline	Hyaline	Black	Hyaline
F8	Skin	Skin, rarely in flesh <sup>a</sup>	Skin, rarely in flesh	Skin, rarely in flesh	90	120	120	180	19.7	28.3	26.5	24.7	Black, pink, hyaline	Black, pink	Black, pink, hyaline	Black
F19	Skin	Skin, rarely in flesh	Skin, rarely in flesh	Skin, rarely in flesh	120	120	120	120	17.3	27.7	26.5	22.9	Hyaline	Black	Black, pink, hyaline	Black
F60	Skin	Skin, rarely in flesh	Skin, rarely in flesh	Skin	120	180	180	180	15.2	24.4	25.9	24.4	Hyaline	Hyaline	Black, pink	Black, pink
PNV1	Skin	Skin, rarely in flesh	Skin, rarely in flesh	Skin, rarely in flesh	180	180	180	210	19.1	25	26.2	27.4	Hyaline	Black	Black	Black, hyaline

RS1	Skin	Skin	Skin	Skin	90	120	120	180	23.8	25.9	24.1	22.6	Black	Black	Black	Black
RS2	Skin	Skin	Skin	Skin	120	210	210	250	18.5	21.2	24.1	10.4	Black, pink and hyaline	Hyaline	Black, pink, hyaline	Pink, hyaline
RS4	Skin	Skin, rarely in flesh	Skin, rarely in flesh	Skin	120	180	180	210	17.9	26.5	26.2	29.8	Hyaline	Black, pink, hyaline	Black, pink, hyaline	Black, pink, hyaline
PFUTa lca27	Skin	Skin	Skin	Skin	120	180	180	210	15.2	23.5	26.8	13.7	Hyaline	Black	Black, pink	Black
ZOF3	Skin	Skin	Skin	Skin	90	120	120	180	23.5	28	24.7	23.5	Black	Black	Black, hyaline	Black
<i>P. vagabunda</i> (morphotype II)																
F13	Skin, flesh	Skin, flesh, core <sup>b</sup>	Skin, flesh, core	Skin, flesh	90	120	120	120	26.5	26.8	25.9	25.3	Black, hyaline	Black	Black, hyaline	Black
F14A	Skin, flesh	Skin, flesh, core	Skin, flesh, core	Skin, flesh	90	120	120	120	27.7	27	27.1	26.8	Black, hyaline	Black	Black	Black
ID02	Skin, flesh	Skin, flesh, core	Skin, flesh, core	Skin, flesh	90	120	120	120	20.1	25.5	27.7	26.5	Hyaline	Black, hyaline	Black, pink	Black

*N. kienholzii*

NK1	Skin, rarely in flesh	Skin, rarely in flesh	Skin, rarely in flesh	Skin	90	120	120	180	11.9	11.6	10.7	8.3	Black, hyaline	Black, hyaline	Black, pink, hyaline	Black, hyaline
-----	-----------------------	-----------------------	-----------------------	------	----	-----	-----	-----	------	------	------	-----	----------------	----------------	----------------------	----------------

*Note.* Kaiser’ pear (K), Golden Delicious (GD), Cripps Pink (CP) and Granny Smith(GS) apples were wounded, infected with conidial suspensions of the pathogens (10<sup>4</sup>conidia/ml) and stored at 0°C. dpi: days postinoculation.

<sup>a</sup>Hypanthium.

<sup>b</sup>Mesocarp.